Electronic Supplementary Material (ESI) for Materials Advances.

Supporting Information for:

Aerosol deposition of porous metal-organic materials onto diverse solid supports

Christine M. Montone[a] and Eric D. Bloch[a]

[a] Department of Chemistry, Indiana University, Bloomington, Indiana 47405, United States

List of Contents

Detailed Experimental Procedures

General Considerations. All reagents were obtained from commercial vendors and used without purification. Low-pressure N_2 & CO_2 adsorption measurements were obtained on a Micromeritics Tristar II PLUS or Micromeritics Tristar 3000. Powder X-ray Diffraction patterns were obtained using a Bruker D8 XRD with a Cu Kα radiation (1.54 nm). Scanning Electron Microscopy images and Energy-Dispersive X-ray spectra were obtained using an SEM/FIB Auriga 60 housed in the Keck Microscopy Suite at the University of Delaware. TGA measurements were obtained using a TA Q5000 SA instrument. Infrared spectra were obtained using a Bruker ALPHA II ATR instrument.

Synthesis of $[Zr_{12}(\mu_3\text{-}O)_4(\mu\text{-}OH)_{12}(Cp)_{12}(m\text{-}bdc)_6]Cl_4$
Material was synthesized according to previously published methods.[1]

Synthesis of $Cu_{24}(5\text{-}undecoxy\text{-}bdc)_{24}$
Material was synthesized according to previously published methods.[2]

Synthesis of UiO-66 nanoparticles
Materials were synthesized according to previously published methods.[3]

Synthesis of HKUST-1
Material was synthesized according to previously published methods.[4]

Synthesis of Fe MIL-101
Material was synthesized according to previously published methods.[5]

Generally, coatings were applied by aerosolizing materials that were either dissolved or suspended in methanol. Aerosolization was carried out by an Aerogen nebulizer utilizing a piezo ring-driven metal mesh aperture vibrating at ultrasonic frequency.

Gas Adsorption Isotherms

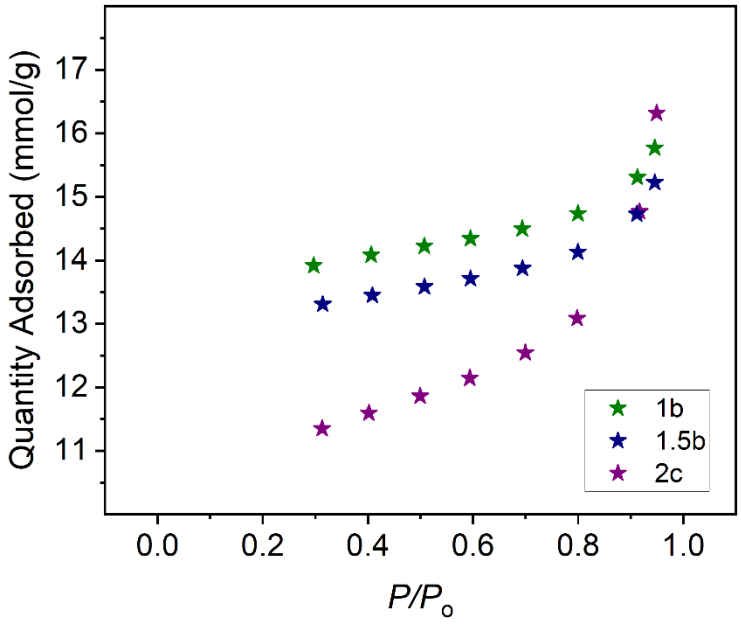

Figure S1. Adsorption of N_2 in bulk UiO-66 nanoparticles 1b (71nm), 1.5b (63nm), and 2c (34 nm) at 77K.

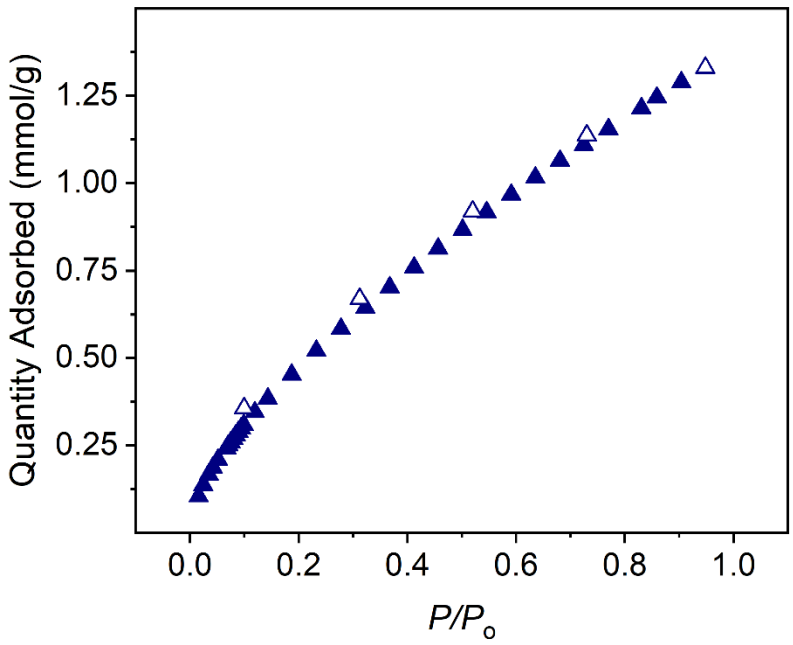

Figure S2. Adsorption of CO_2 in bulk UiO-66 1b (34nm) nanoparticles at 313K. = TGA = 0.697 mmol/g aerosol = 0.347 mmol/g

Infrared Spectra

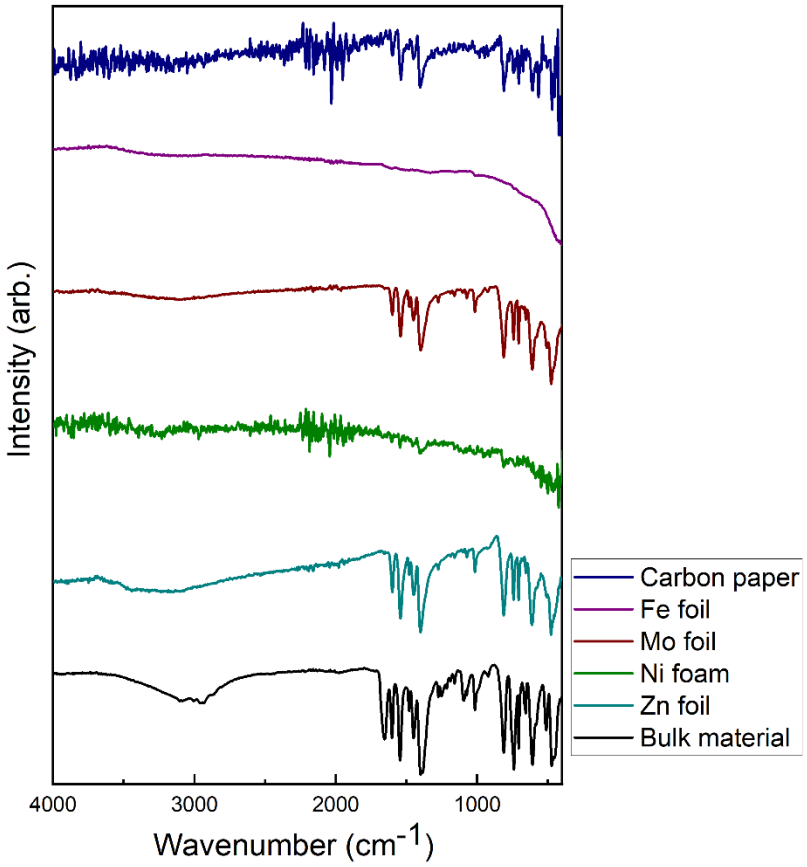

Figure S3. Stacked IR spectra of $[Zr_{12}(\mu_3\text{-}O)_4(\mu_2\text{-}OH)_{12}(Cp)_{12}(m\text{-}bdc)_6]Cl_4$ dissolved in methanol then aerosolized onto surfaces. Of note, the spectra match well in the fingerprint region, indicating the similarity of chemical species between bulk and deposited materials.

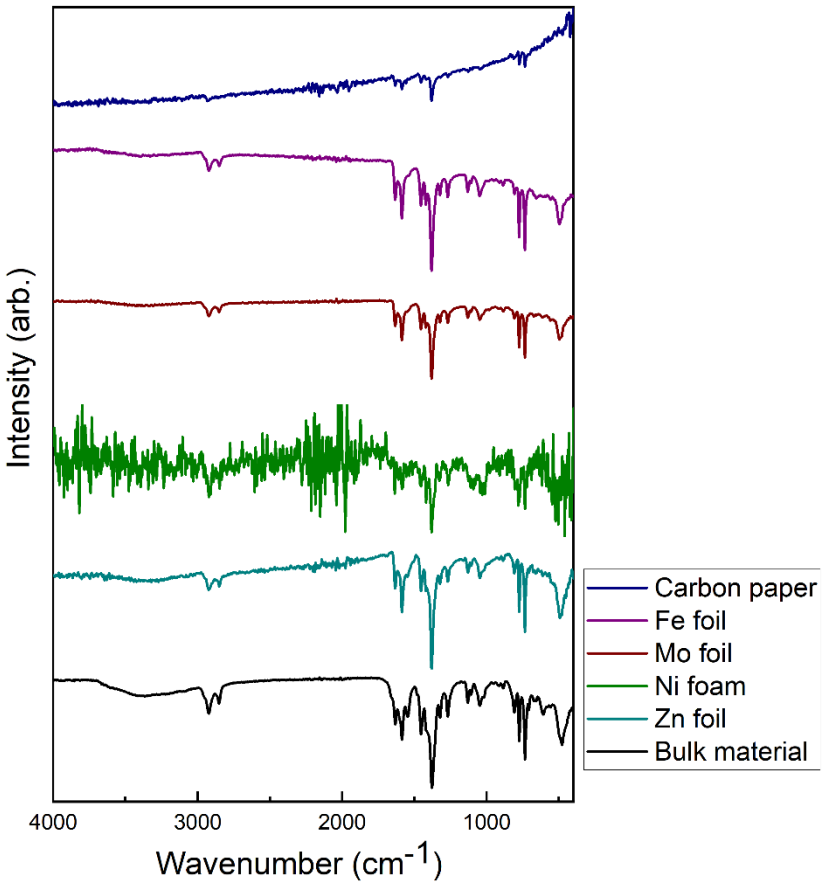

Figure S4. Stacked IR spectra of Cu_{24}(5-undecoxy-bdc)$_{24}$ suspended in methanol then aerosolized onto surfaces. Of note, the spectra match well in the fingerprint region, indicating the similarity of chemical species between bulk and deposited materials.

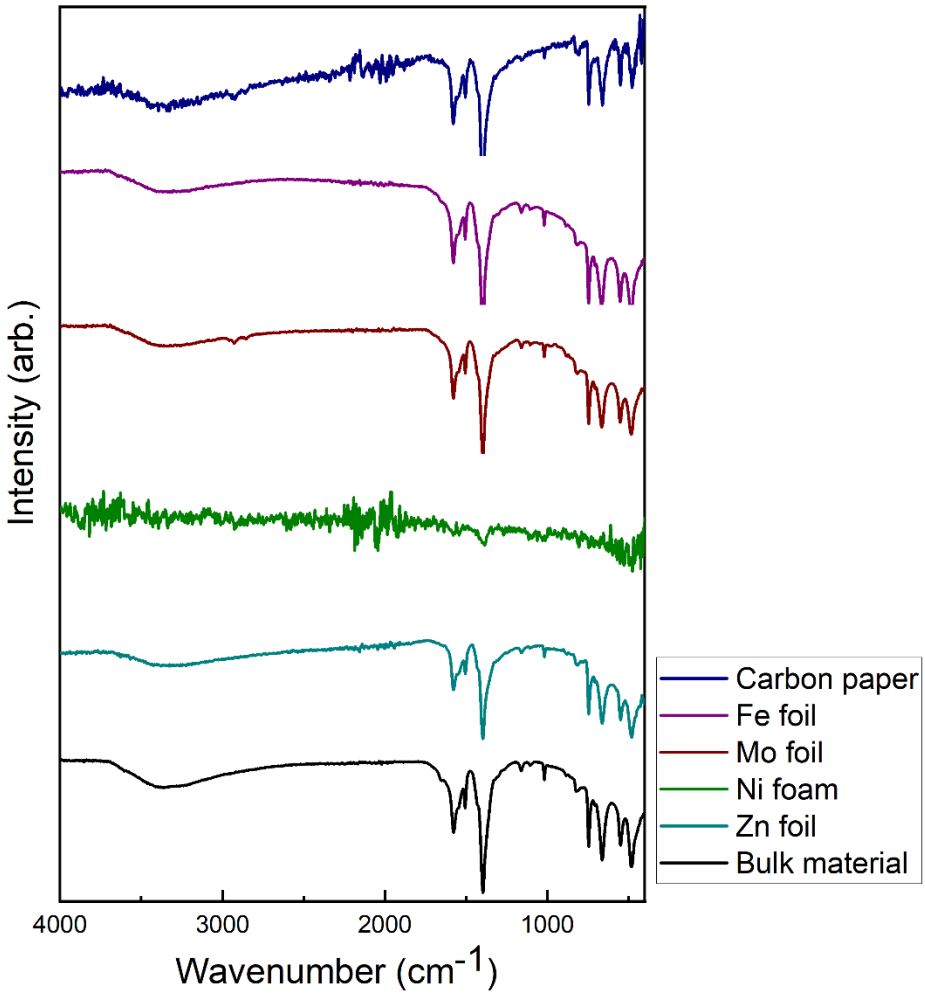

Figure S5. Stacked IR spectra of UiO-66 1b (71nm) nanoparticles suspended in methanol then aerosolized onto surfaces. Of note, the spectra match well in the fingerprint region, indicating the similarity of chemical species between bulk and deposited materials.

Powder X-Ray Diffraction Patterns

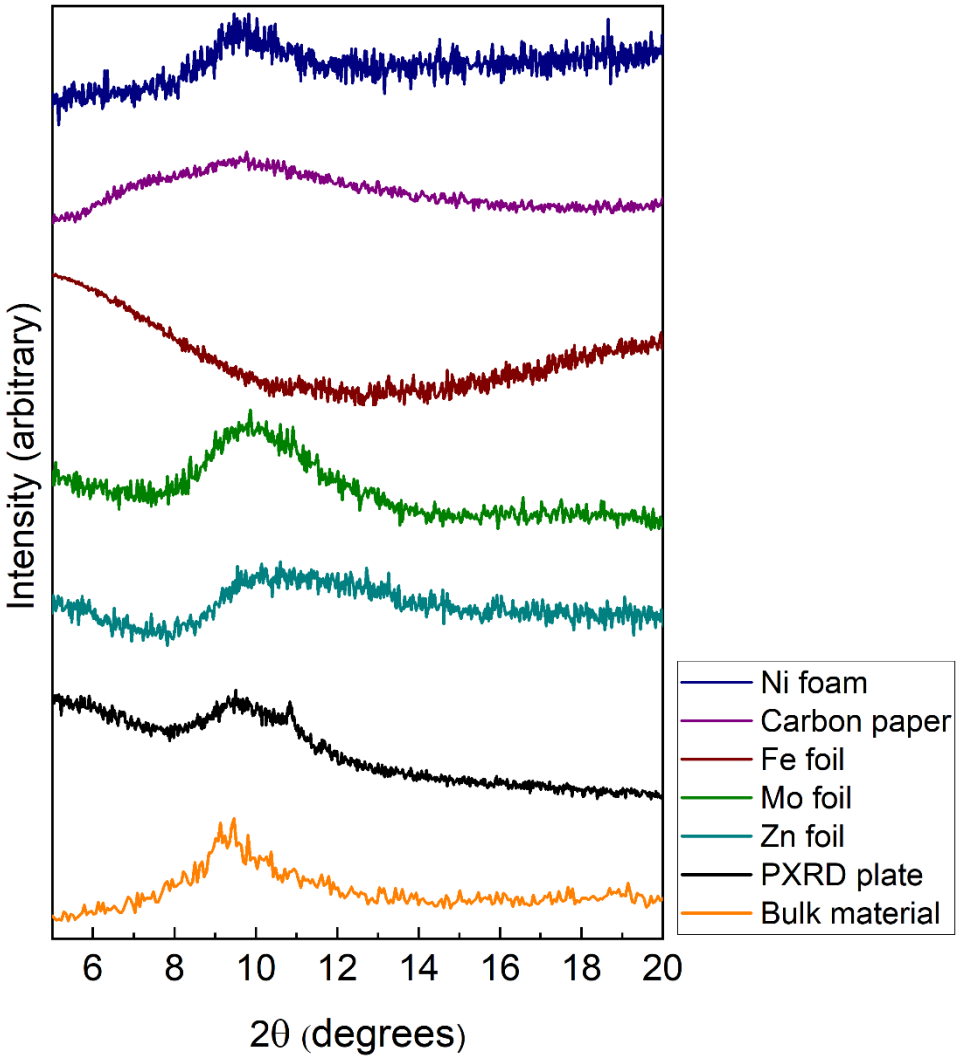

Figure S6. Stacked PXRD patterns of $[Zr_{12}(\mu_3\text{-}O)_4(\mu_2\text{-}OH)_{12}(Cp)_{12}(m\text{-}bdc)_6]Cl_4$ dissolved in methanol then aerosolized onto surfaces.

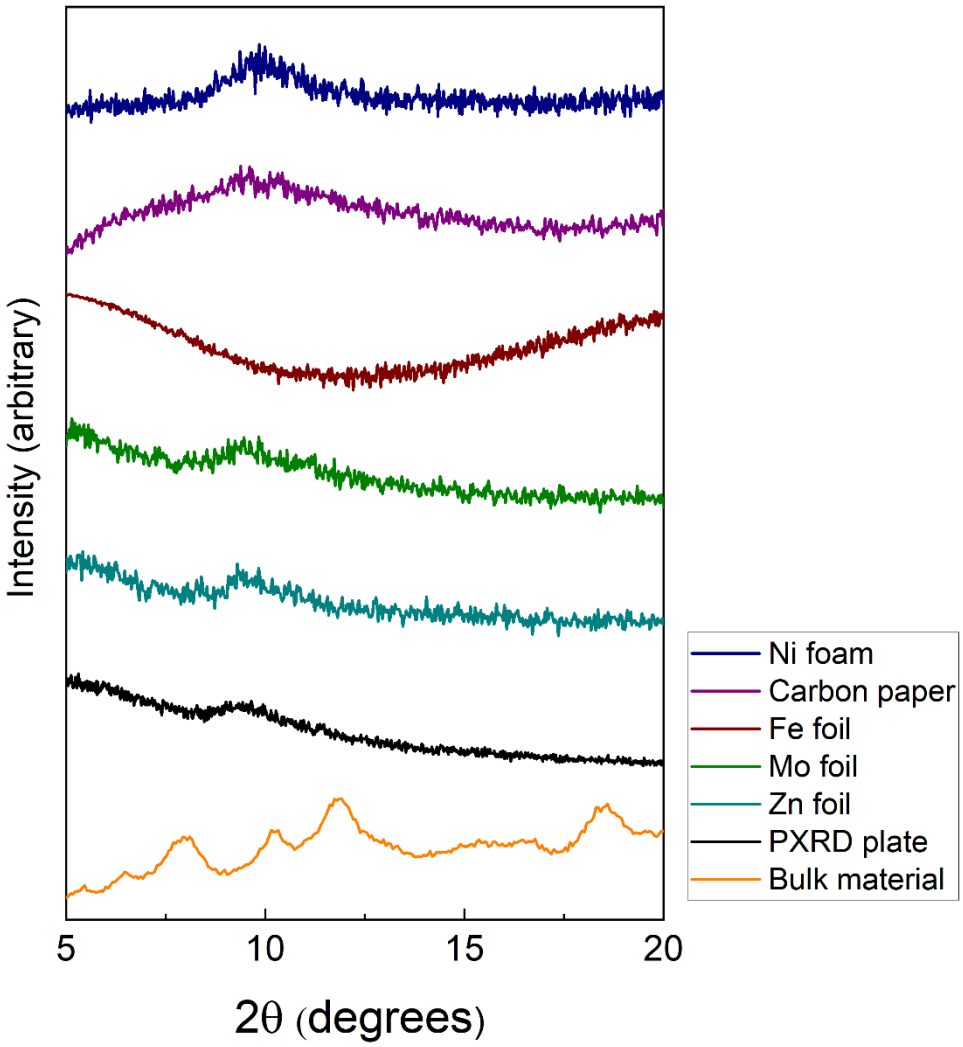

Figure S7. Stacked PXRD patterns of Cu_{24}(5-undecoxy-bdc)$_{24}$ suspended in methanol then aerosolized onto surfaces.

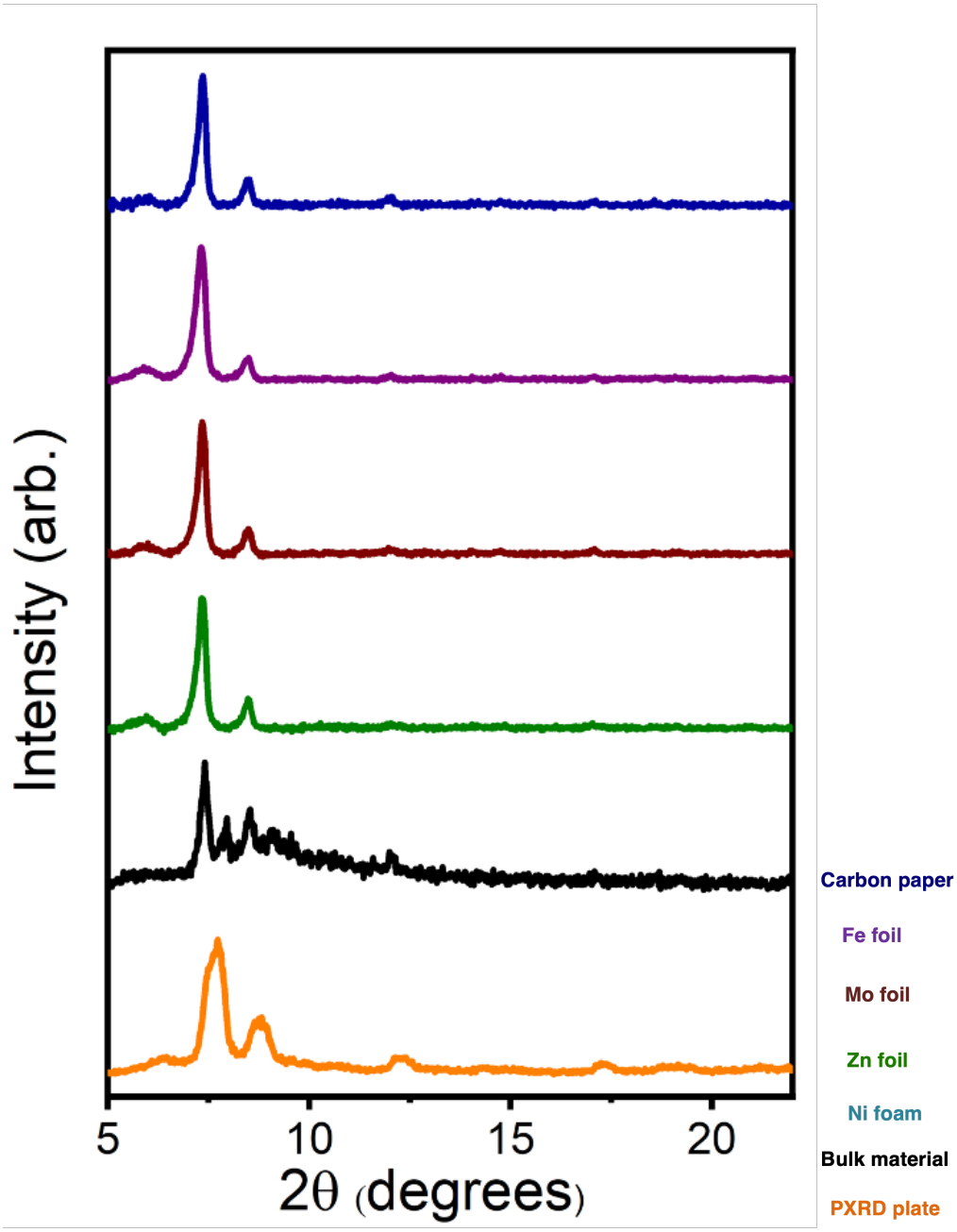

Figure S8. Stacked PXRD patterns of UiO-66 1b (71nm) nanoparticles suspended in methanol then aerosolized onto surfaces.

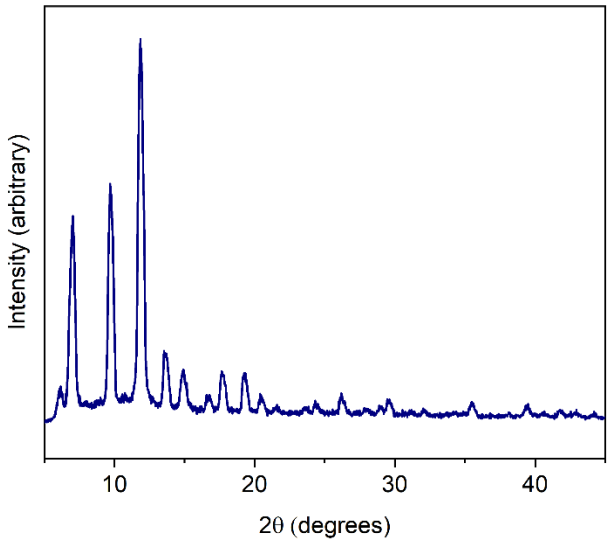

Figure S11. PXRD pattern of HKUST-1 bulk material.

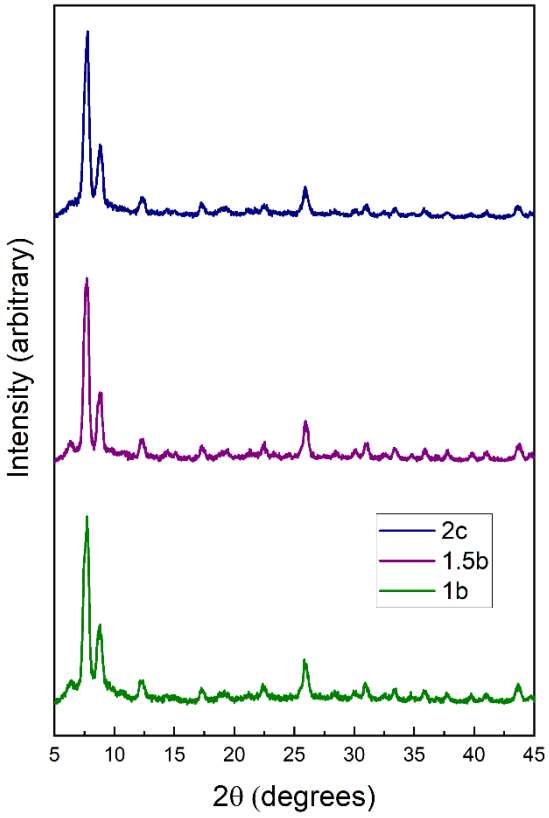

Figure S9. Stacked PXRD patterns of 3 UiO-66 nanoparticles: 1b (71nm), 1.5b (63nm), & 2c (34nm).

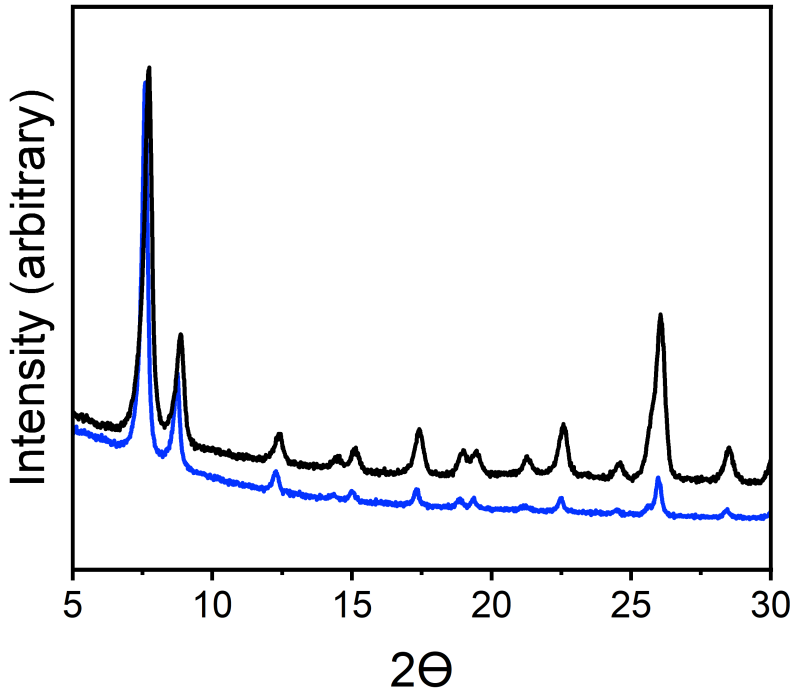

Figure S10. Stacked PXRD patterns of UiO-66 high surface area bulk powder (black) and aerosolized onto Zn foil (blue).

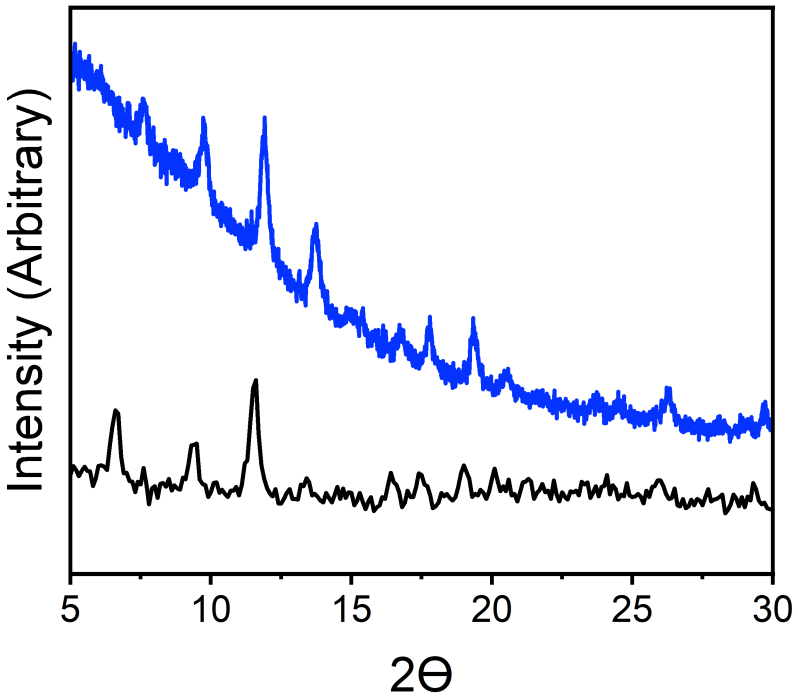

Figure S11. Stacked PXRD patterns of HKUST-1 nanoparticles bulk powder (black) and aerosolized onto Zn foil (blue).

Scanning Electron Microscopy Images & Energy-Dispersive X-ray Spectra

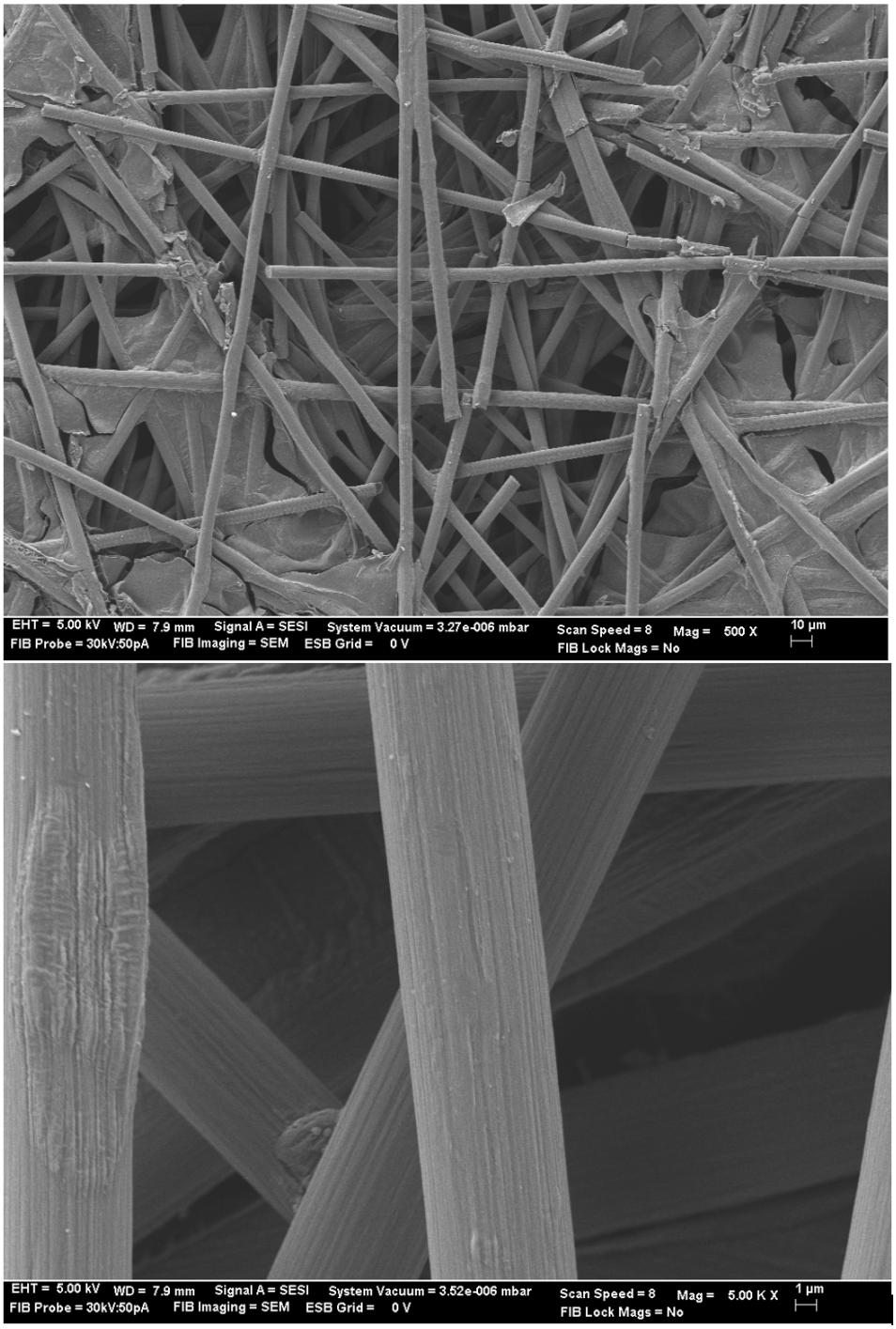

Figure S12. SEM images of carbon paper.

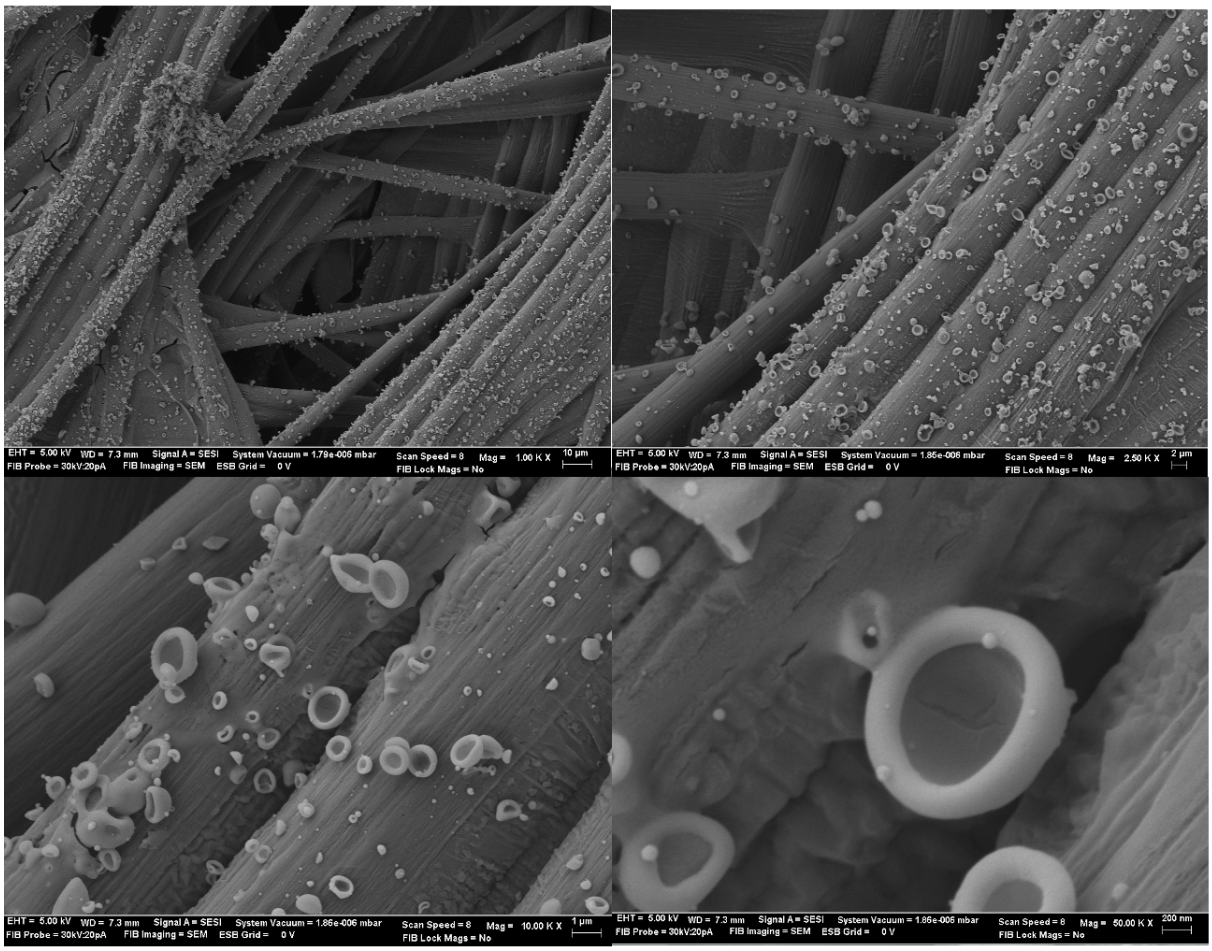

Figure S13. SEM images of $[Zr_{12}(\mu_3\text{-}O)_4(\mu_2\text{-}OH)_{12}(Cp)_{12}(m\text{-}bdc)_6]Cl_4$ dissolved in methanol then aerosolized onto carbon paper.

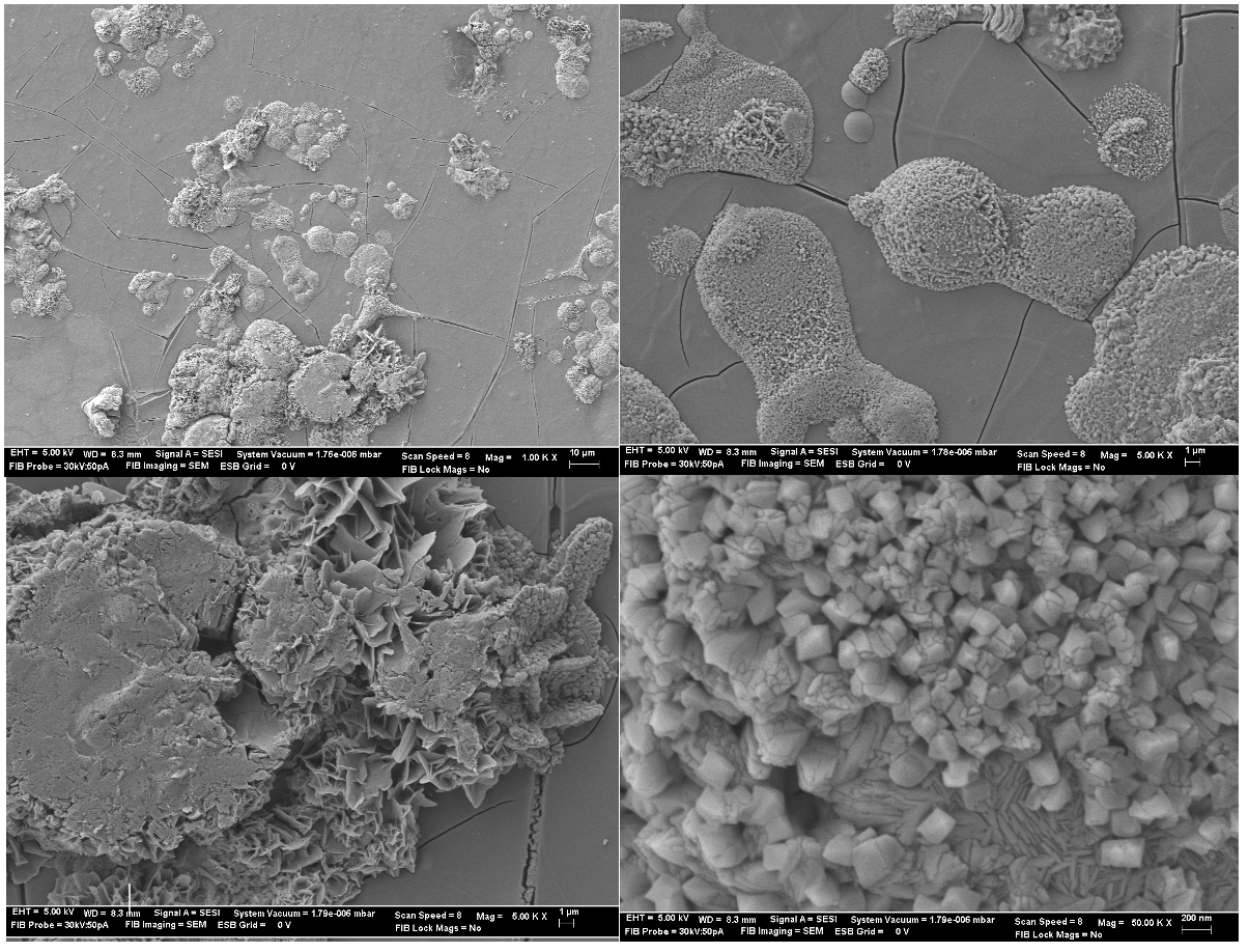

Figure S14. SEM images of $[Zr_{12}(\mu_3\text{-}O)_4(\mu_2\text{-}OH)_{12}(Cp)_{12}(m\text{-}bdc)_6]Cl_4$ dissolved in methanol then aerosolized onto iron foil.

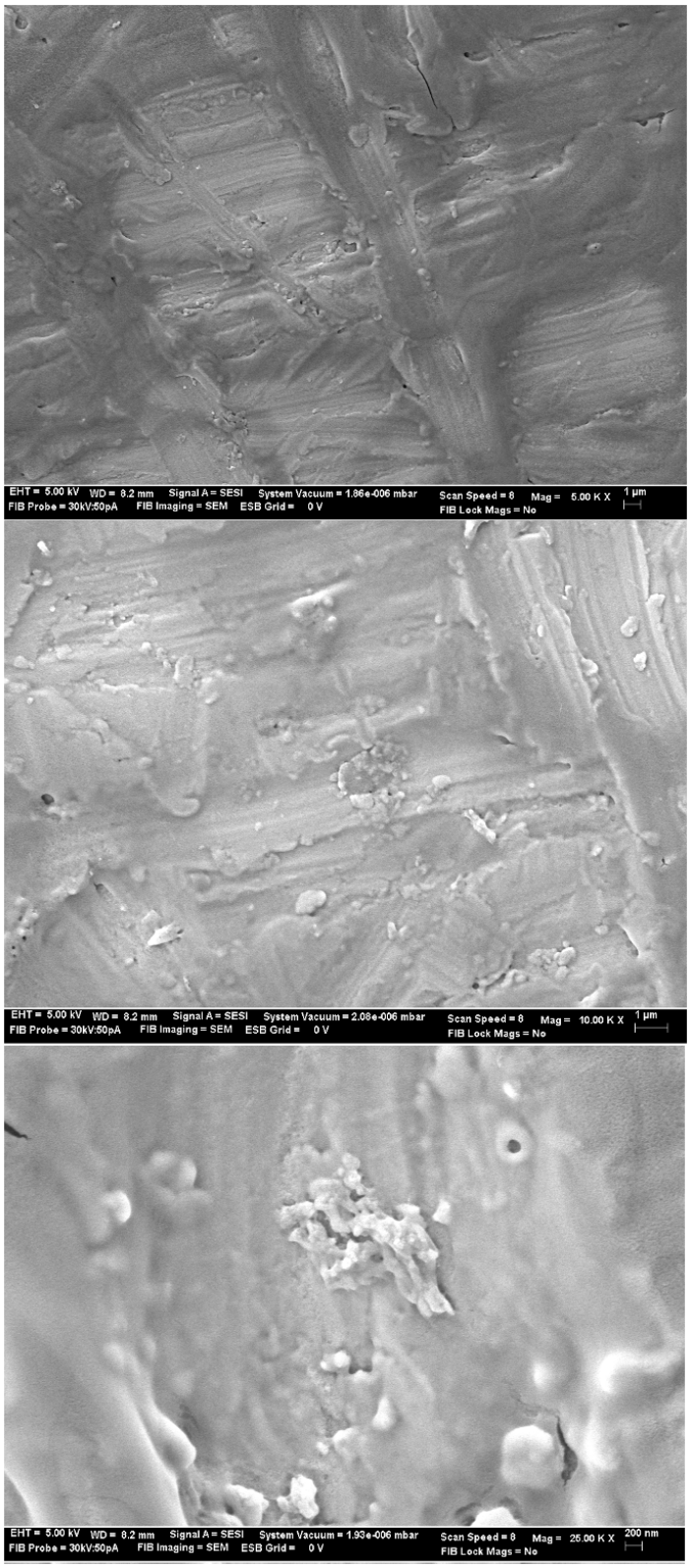

Figure S15. SEM images of $[Zr_{12}(\mu_3\text{-}O)_4(\mu_2\text{-}OH)_{12}(Cp)_{12}(m\text{-}bdc)_6]Cl_4$ dissolved in methanol then aerosolized onto molybdenum foil.

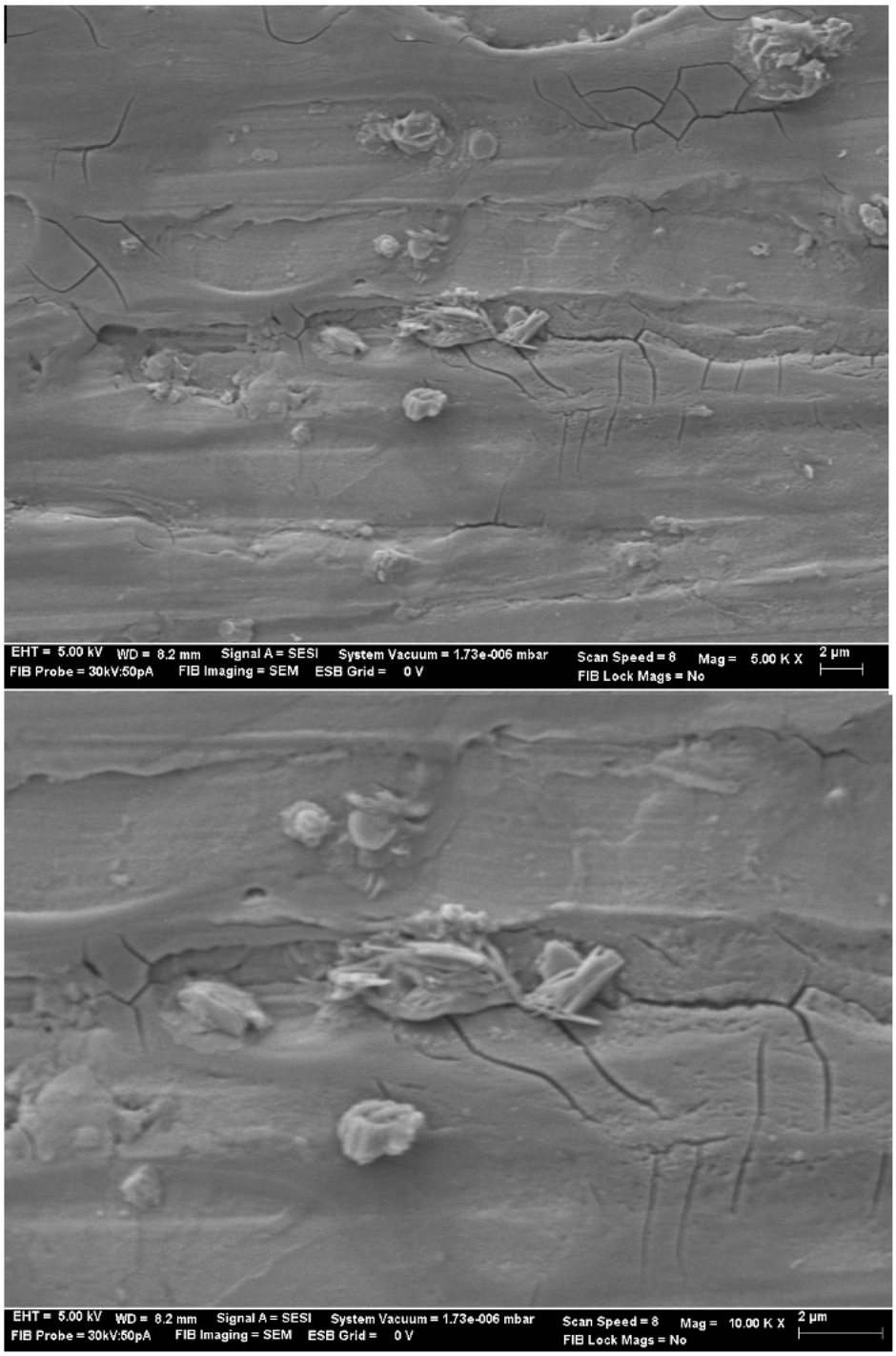

Figure S16. SEM images of $[Zr_{12}(\mu_3\text{-}O)_4(\mu_2\text{-}OH)_{12}(Cp)_{12}(m\text{-}bdc)_6]Cl_4$ dissolved in methanol then aerosolized onto zinc foil.

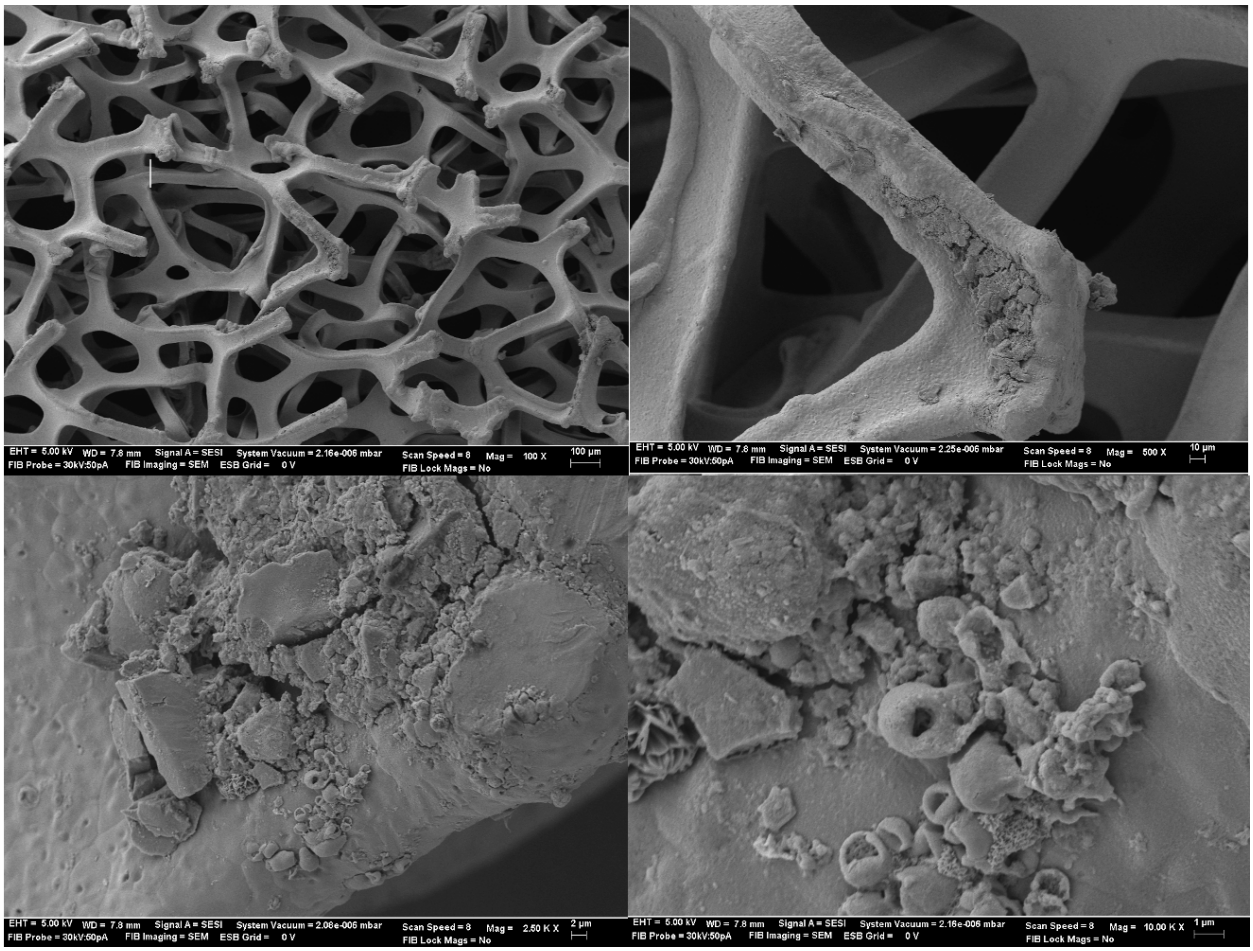

Figure S17. SEM images of $[Zr_{12}(\mu_3\text{-}O)_4(\mu_2\text{-}OH)_{12}(Cp)_{12}(m\text{-}bdc)_6]Cl_4$ dissolved in methanol then aerosolized onto nickel foam.

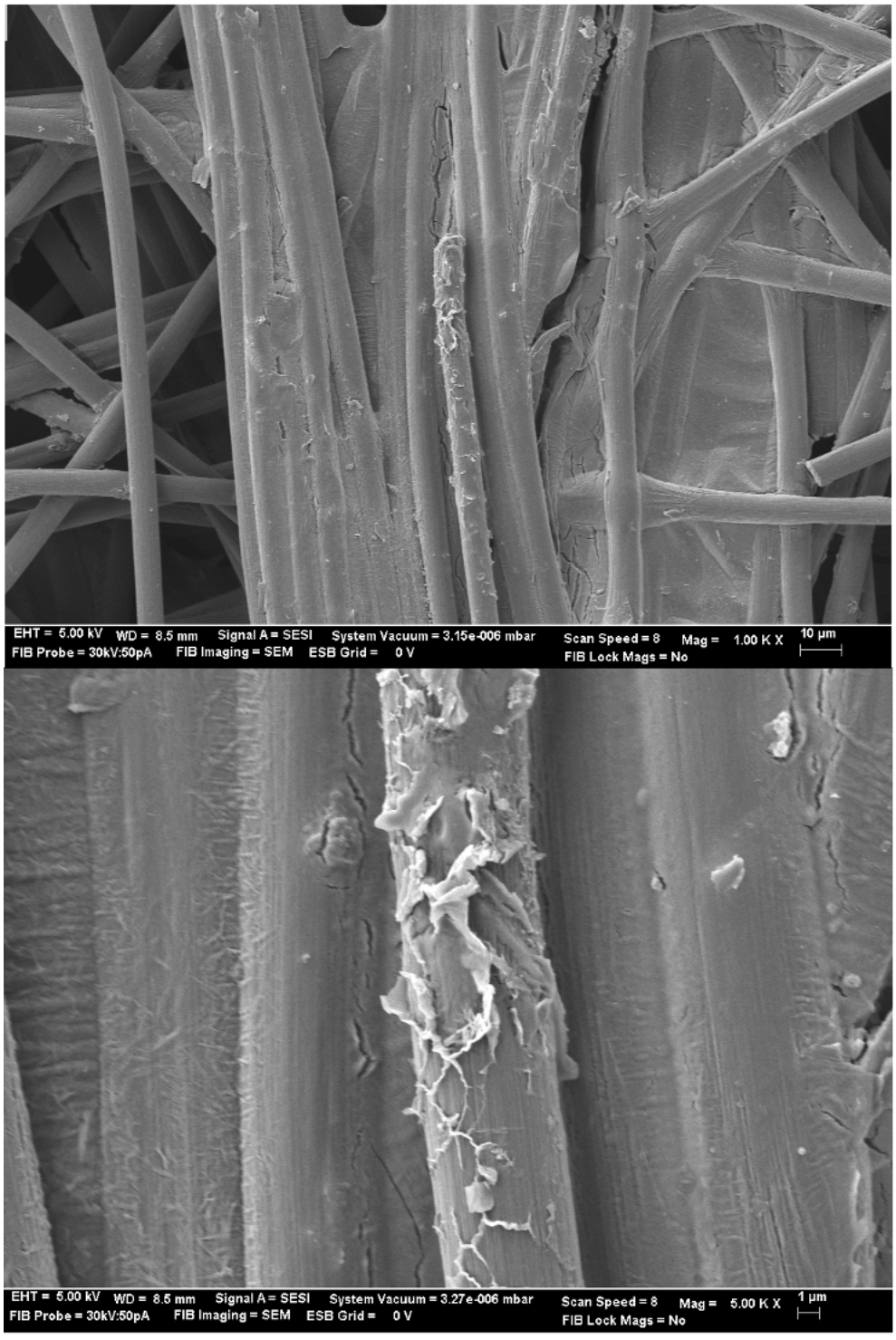

Figure S18. SEM images of $[Zr_{12}(\mu_3\text{-}O)_4(\mu_2\text{-}OH)_{12}(Cp)_{12}(m\text{-}bdc)_6]Cl_4$ dissolved in methanol then applied dropwise to carbon paper.

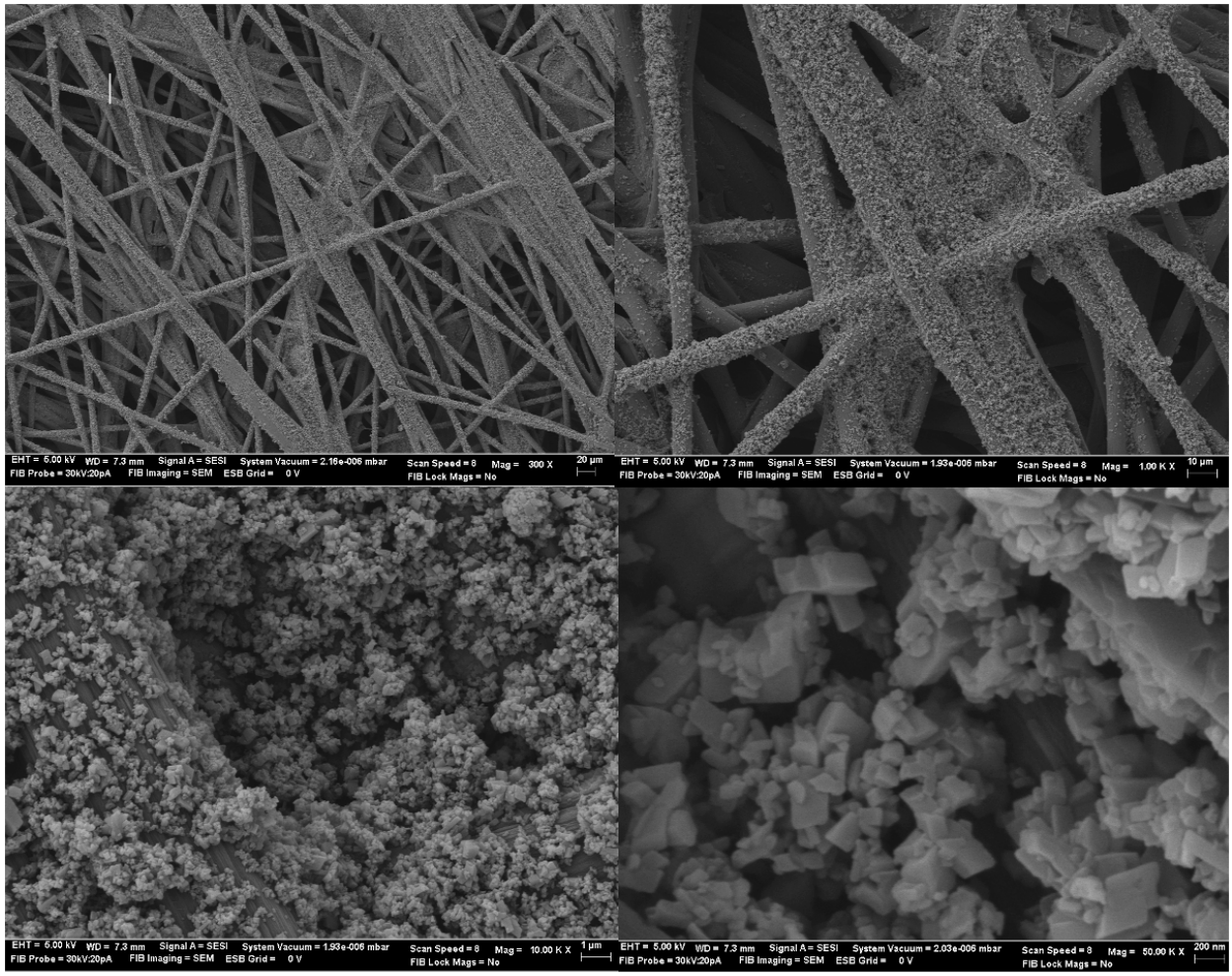

Figure S19. SEM images of Cu_{24}(5-undecoxy-bdc)$_{24}$ suspended in methanol then aerosolized onto carbon paper.

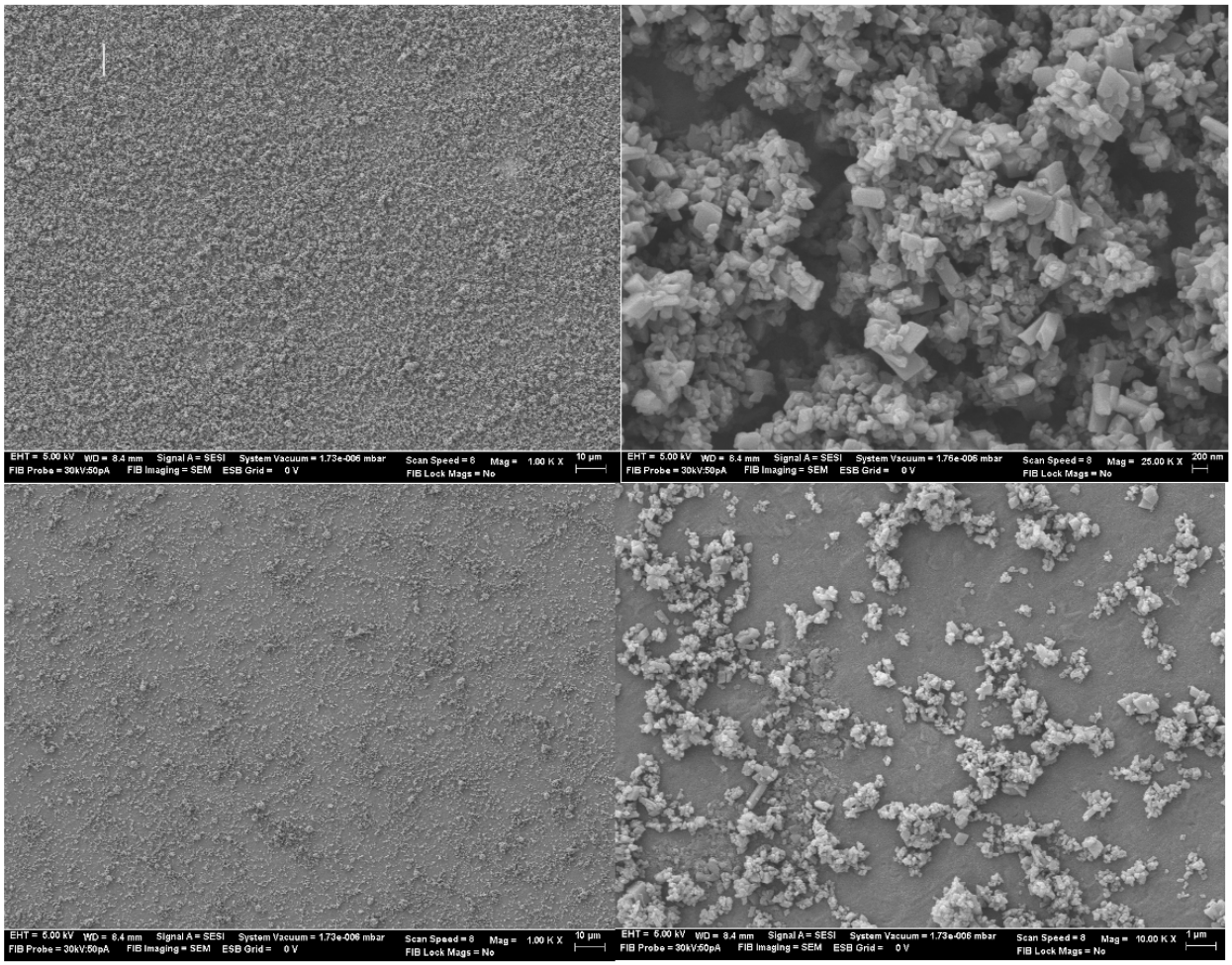

Figure S20. SEM images of Cu_{24}(5-undecoxy-bdc)$_{24}$ suspended in methanol then aerosolized onto iron foil.

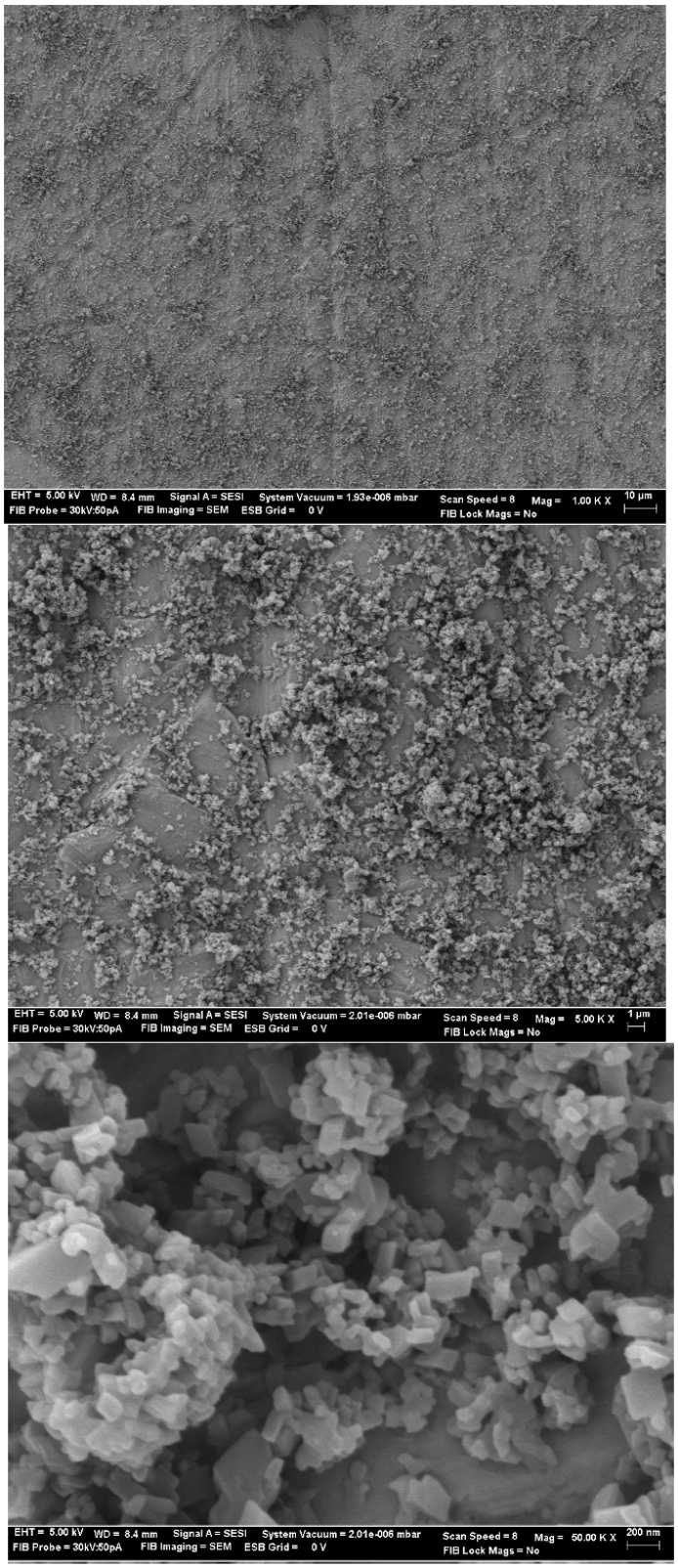

Figure S21. SEM images of Cu_{24}(5-undecoxy-bdc)$_{24}$ suspended in methanol then aerosolized onto molybdenum foil.

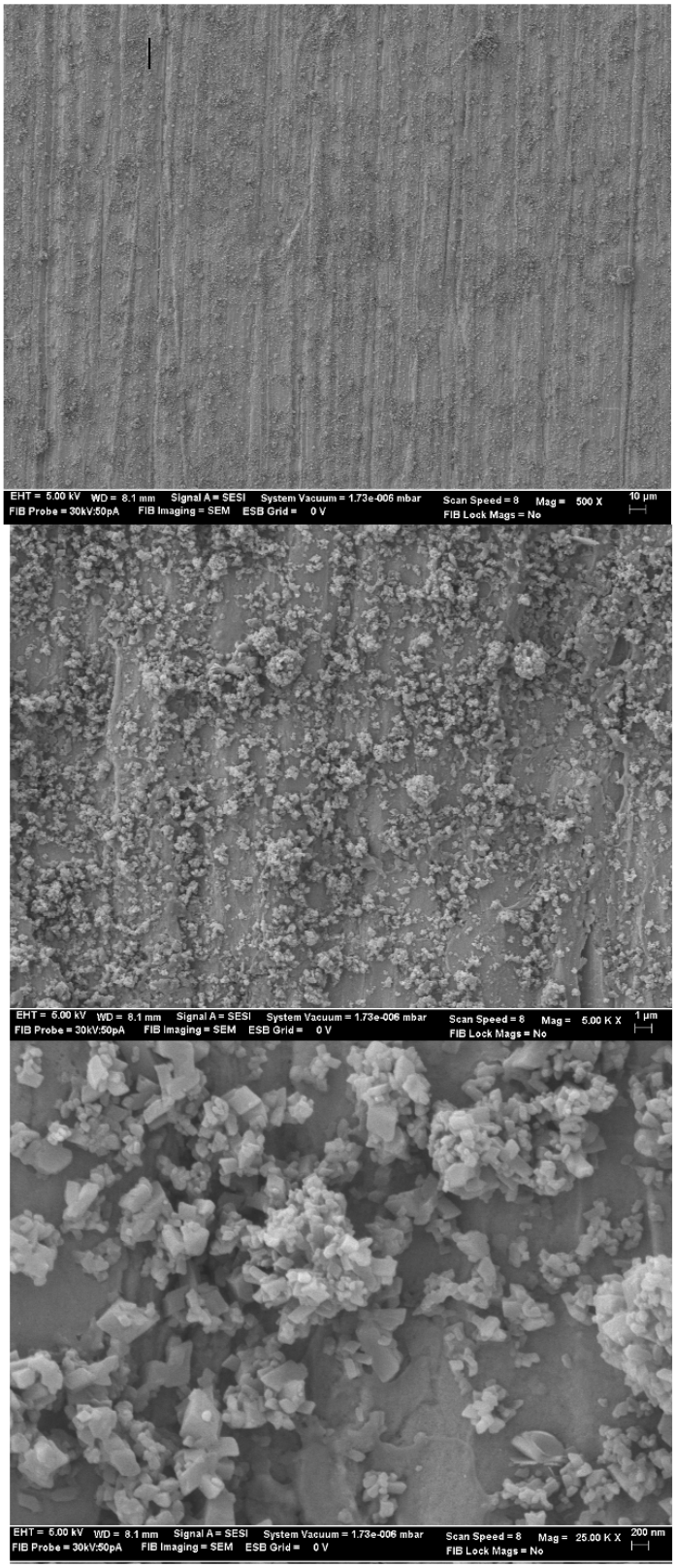

Figure S22. SEM images of Cu_{24}(5-undecoxy-bdc)$_{24}$ suspended in methanol then aerosolized onto zinc foil.

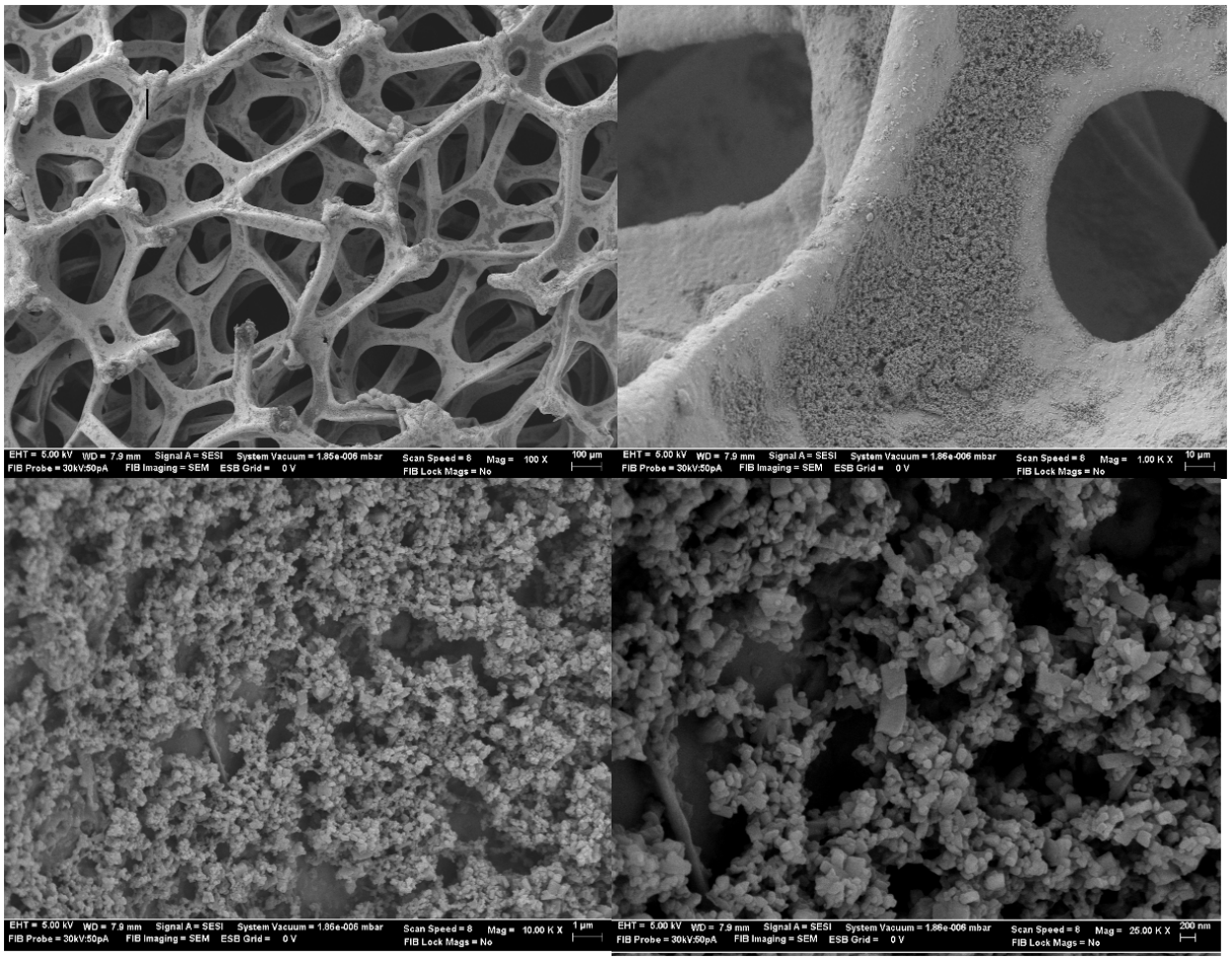

Figure S23. SEM images of Cu_{24}(5-undecoxy-bdc)$_{24}$ suspended in methanol then aerosolized onto nickel foam.

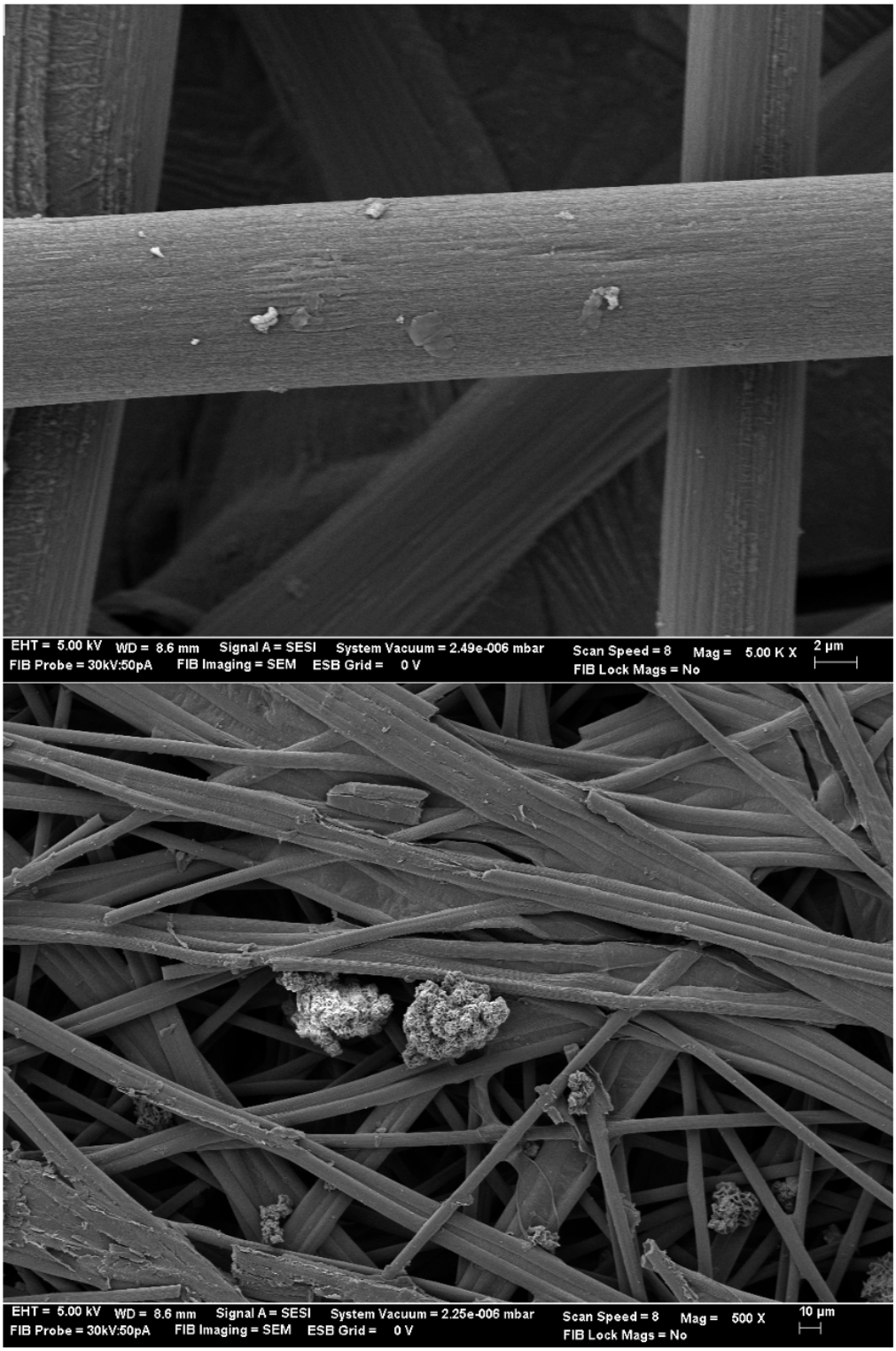

Figure S24. SEM images of Cu_{24}(5-undecoxy-bdc)$_{24}$ suspended in methanol then applied dropwise to carbon paper.

a) b)

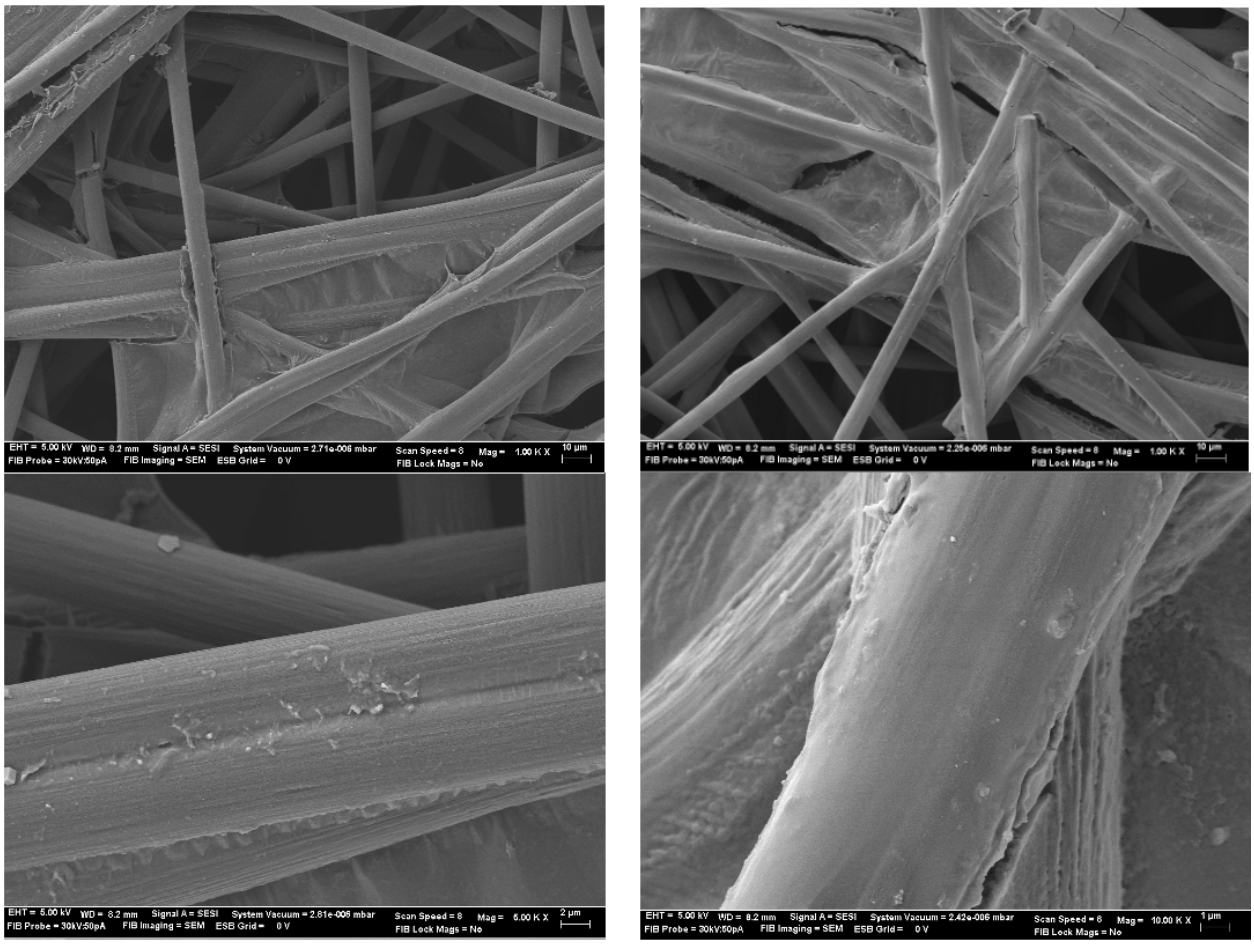

Figure S25. SEM images of $[Zr_{12}(\mu_3\text{-}O)_4(\mu_2\text{-}OH)_{12}(Cp)_{12}(m\text{-}bdc)_6]Cl_4$ dissolved in methanol, aerosolized onto carbon paper, then a) dipped into methanol for 30 seconds and b) sonicated in methanol for 30 seconds.

a) b)

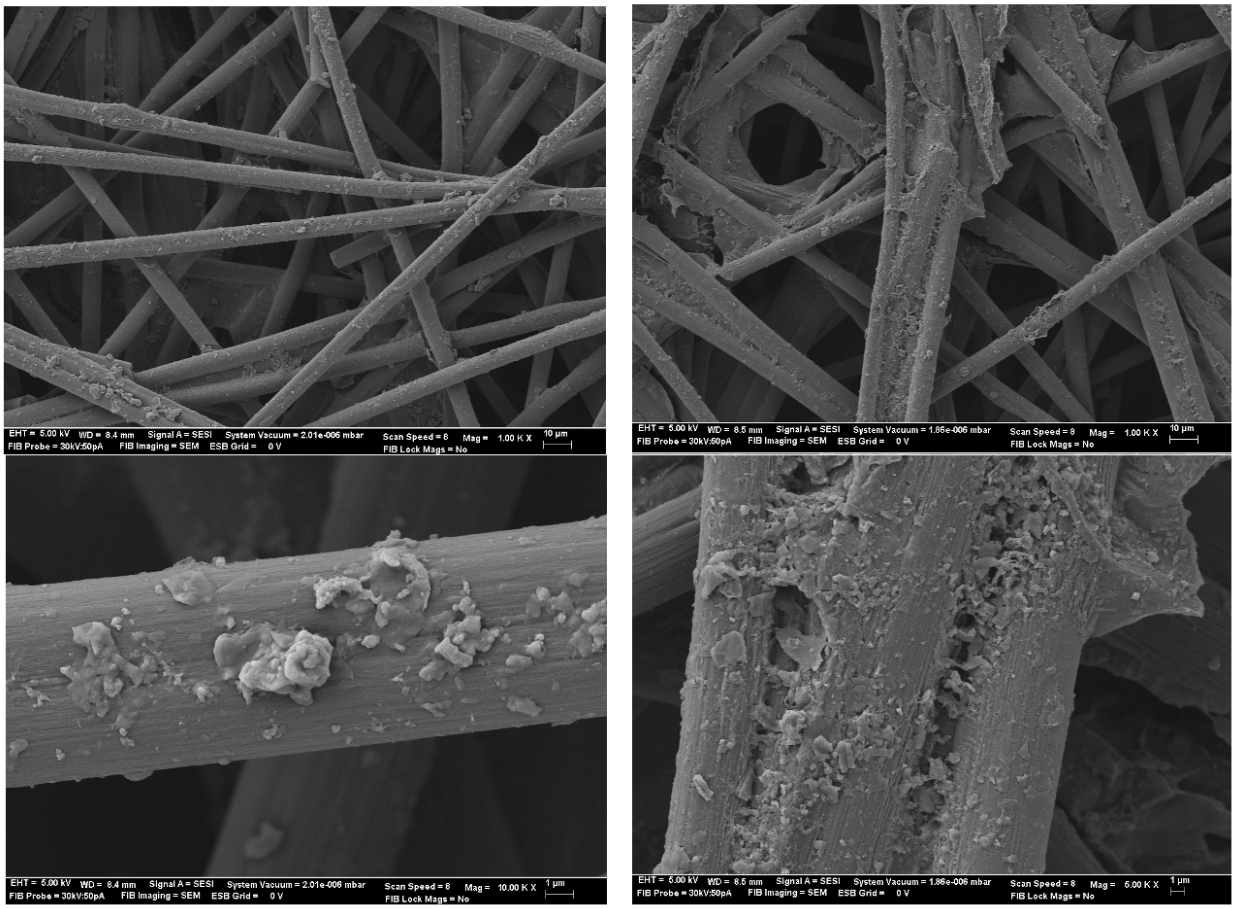

Figure S26. SEM images of Cu_{24}(5-undecoxy-bdc)$_{24}$ suspended in methanol, aerosolized onto carbon paper, then a) dipped into methanol for 30 seconds and b) sonicated in methanol for 30 seconds.

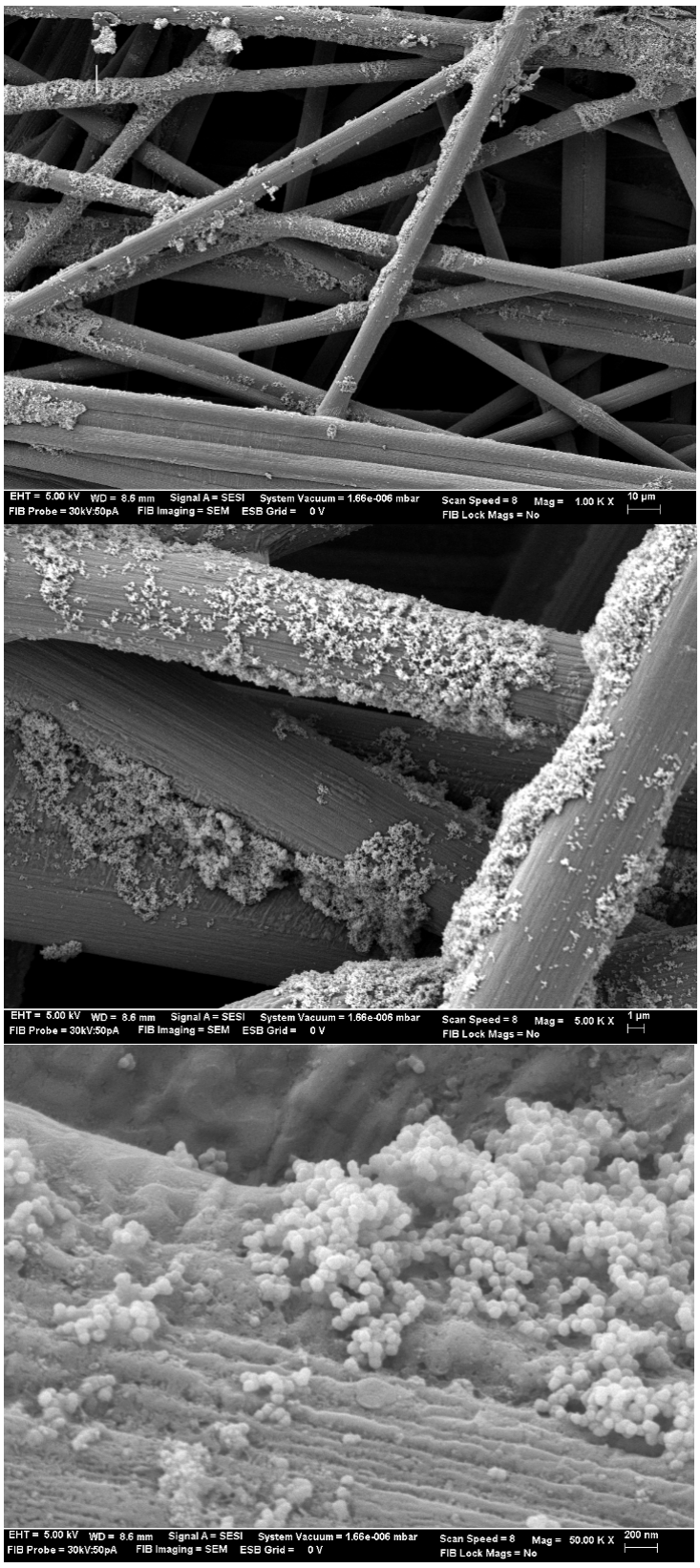

Figure S27. SEM images of UiO-66 1b (71nm) nanoparticles suspended in methanol, aerosolized onto carbon paper, then sonicated in methanol for 5 minutes.

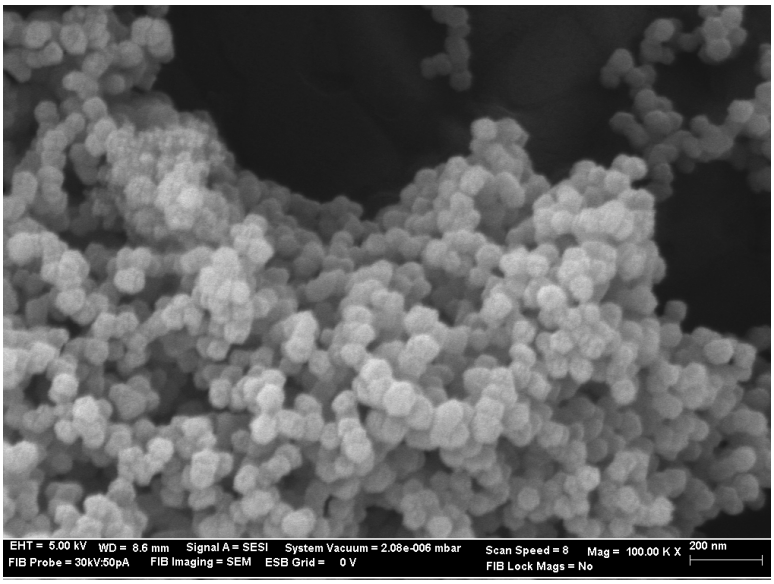

Figure S28. SEM images of UiO-66 1b nanoparticles suspended in methanol then aerosolized onto carbon paper. Following imaging, particles were sized using the ImageJ program, manually selecting fifty particle diameters using the software measurement tool. The average of the fifty particle measurements is 71.4 nm.

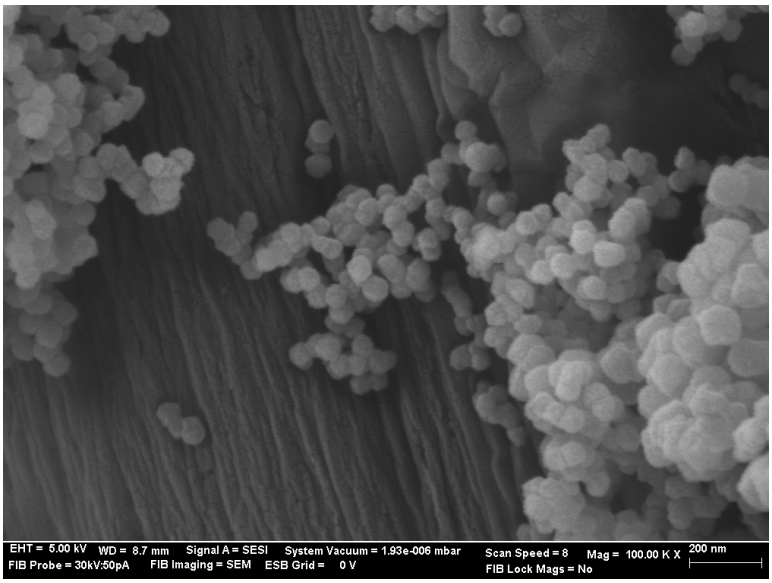

Figure S29. SEM images of UiO-66 1.5b nanoparticles suspended in methanol then aerosolized onto carbon paper. Following imaging, particles were sized using the ImageJ program, manually selecting fifty particle diameters using the software measurement tool. The average of the fifty particle measurements is 62.5 nm.

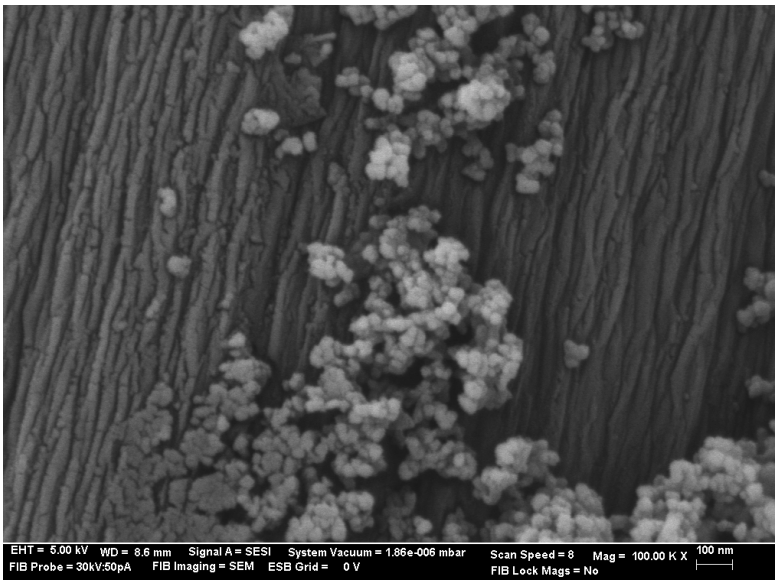

Figure S30. SEM images of UiO-66 2c nanoparticles suspended in methanol then aerosolized onto carbon paper. Following imaging, particles were sized using the ImageJ program, manually selecting fifty particle diameters using the software measurement tool. The average of the fifty particle measurements is 34.0 nm.

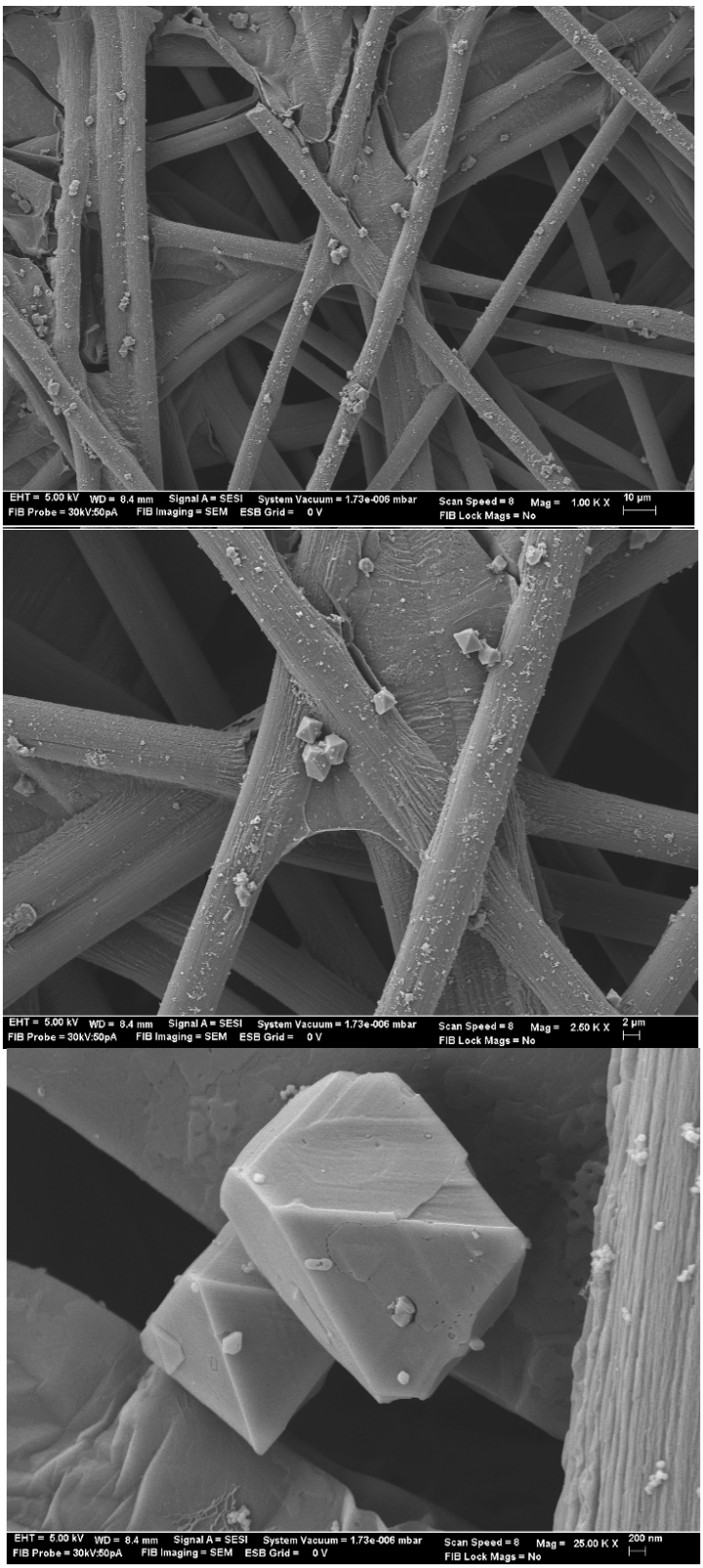

Figure S31. SEM images of HKUST-1 suspended in methanol then aerosolized onto carbon paper.

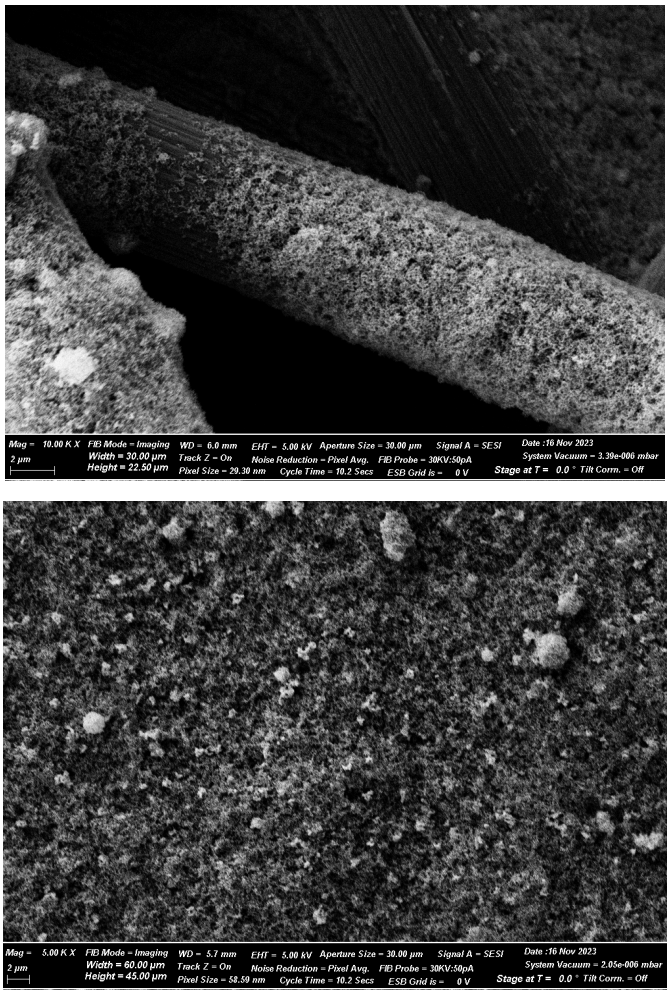

Figure S32. SEM images of HKUST-1 nanoparticles suspended in ethanol then aerosolized onto carbon paper (top) and Zn foil (bottom.)

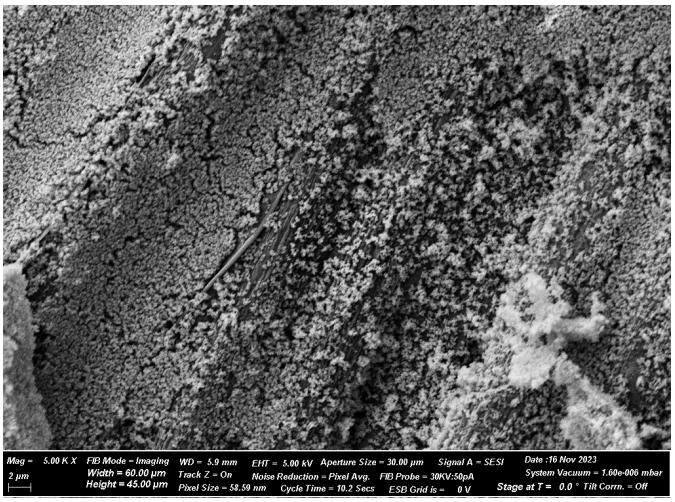

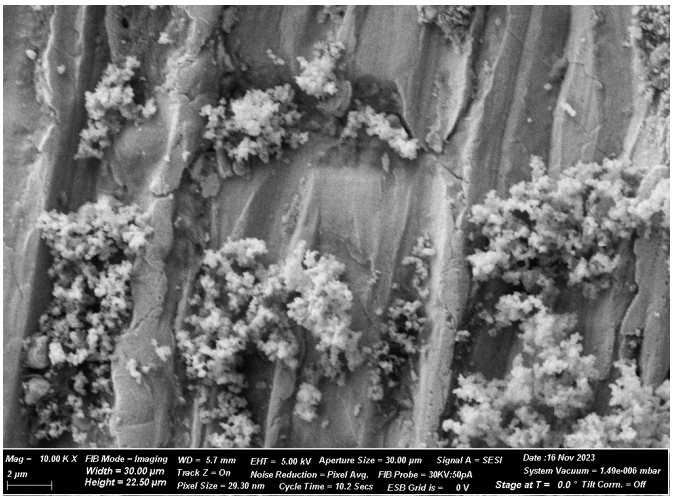

Figure S33. SEM images of UiO-66 high surface area suspended in methanol then aerosolized onto carbon paper (top) and Zn foil (bottom.)

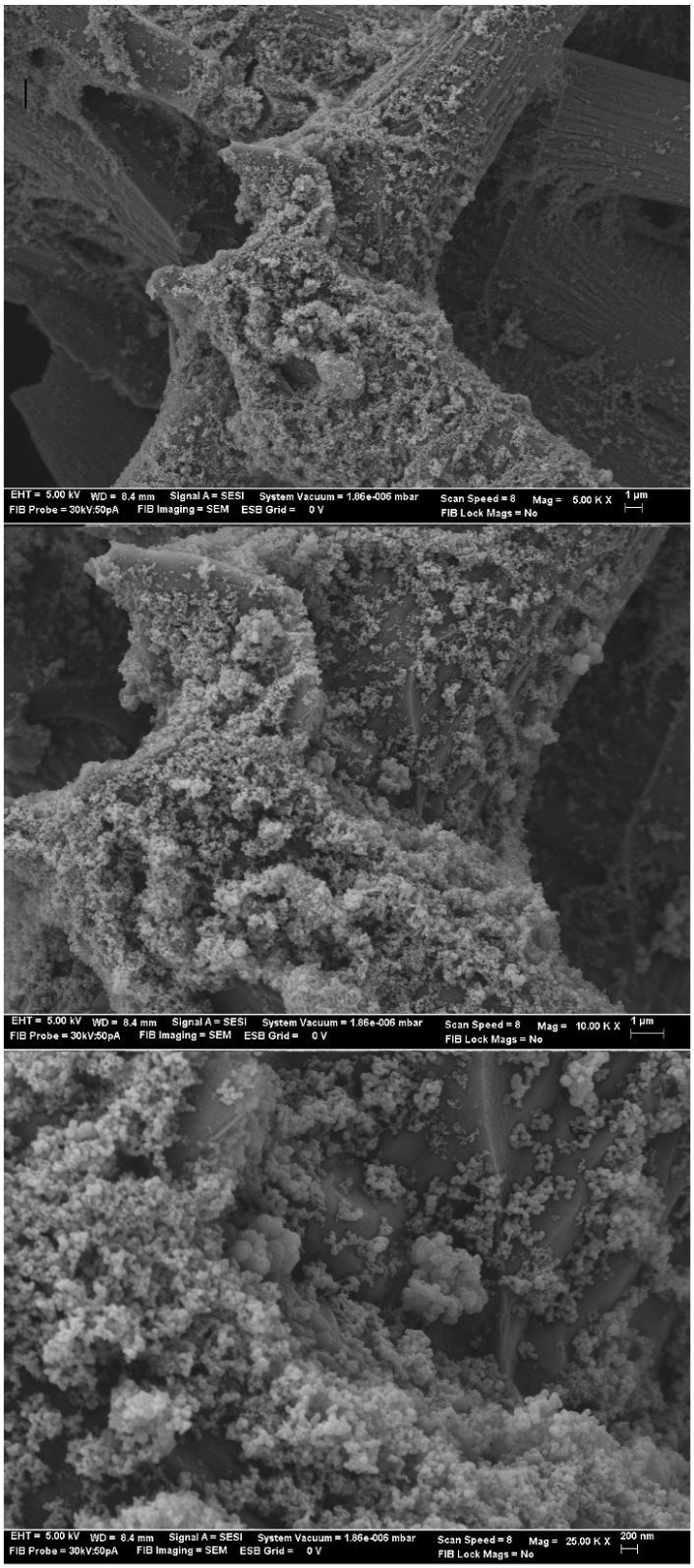

Figure S34. SEM images of UiO-66 1b (71nm), 1.5b (63nm), & 2c (34nm) mixed nanoparticles suspended in methanol then aerosolized onto carbon paper.

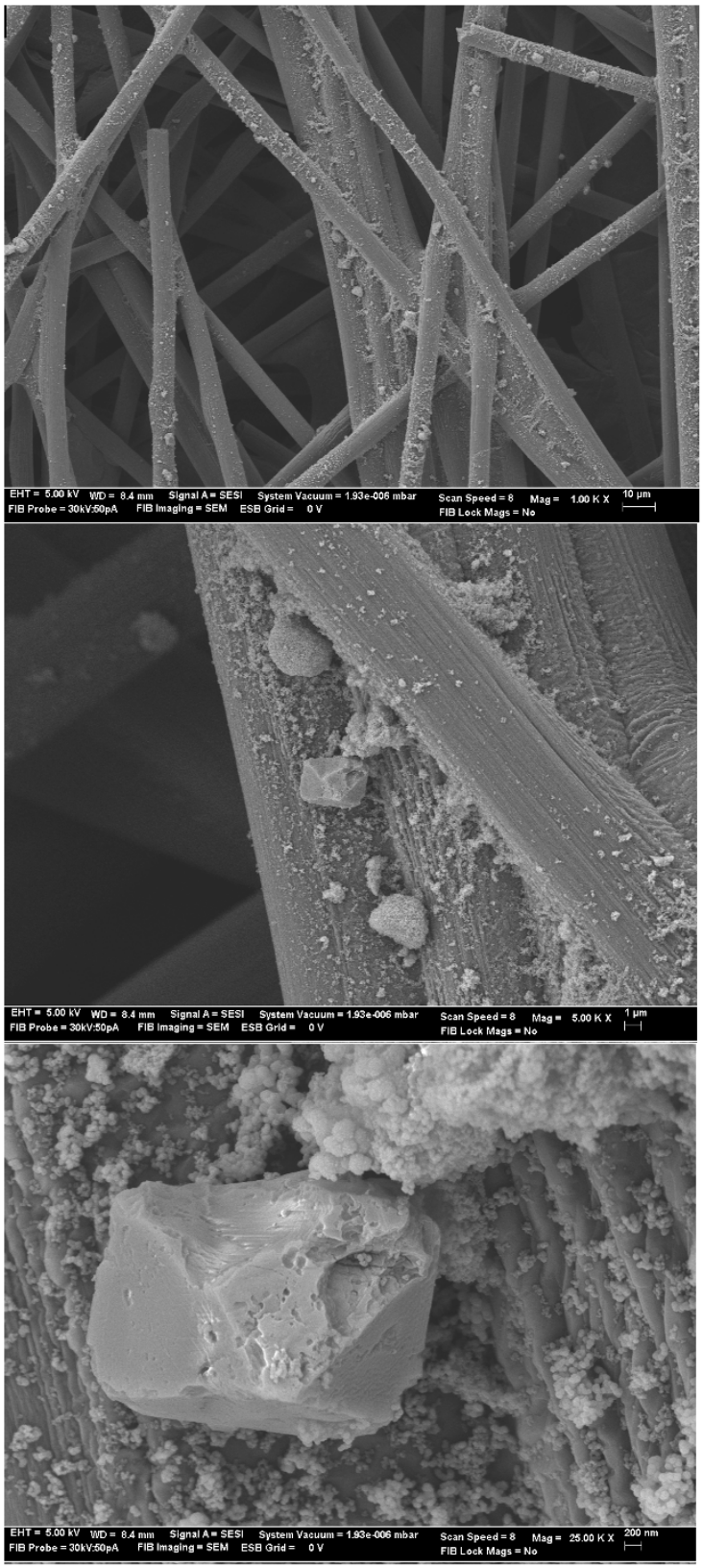

Figure S35. SEM images of UiO-66 1b (71nm), 1.5b (63nm), 2c (34nm), & HKUST-1 particles suspended in methanol then aerosolized onto carbon paper.

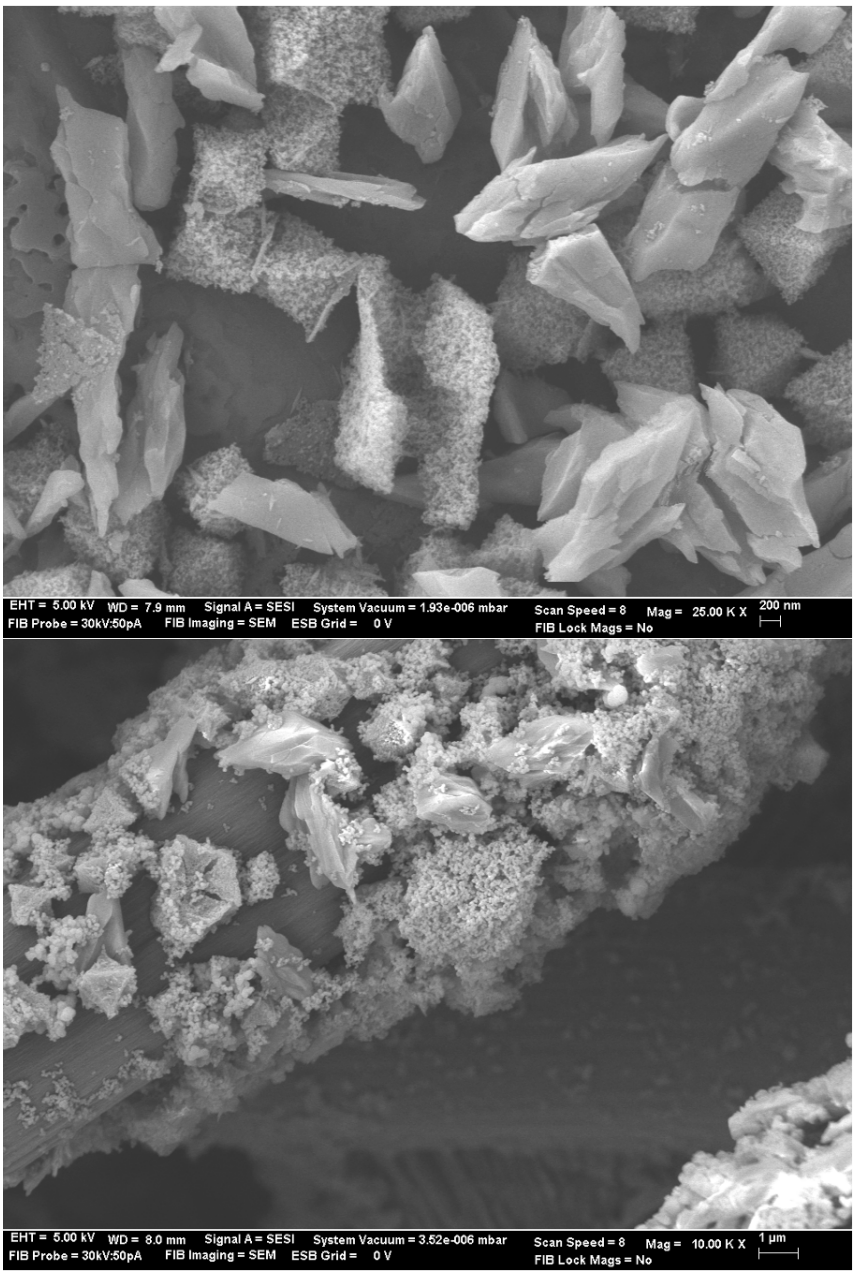

Figure S36. SEM images of (top) Fe MIL-101 & (bottom) UiO-66 1.5b (63nm) & Fe MIL-101 particles suspended in methanol then aerosolized onto carbon paper.

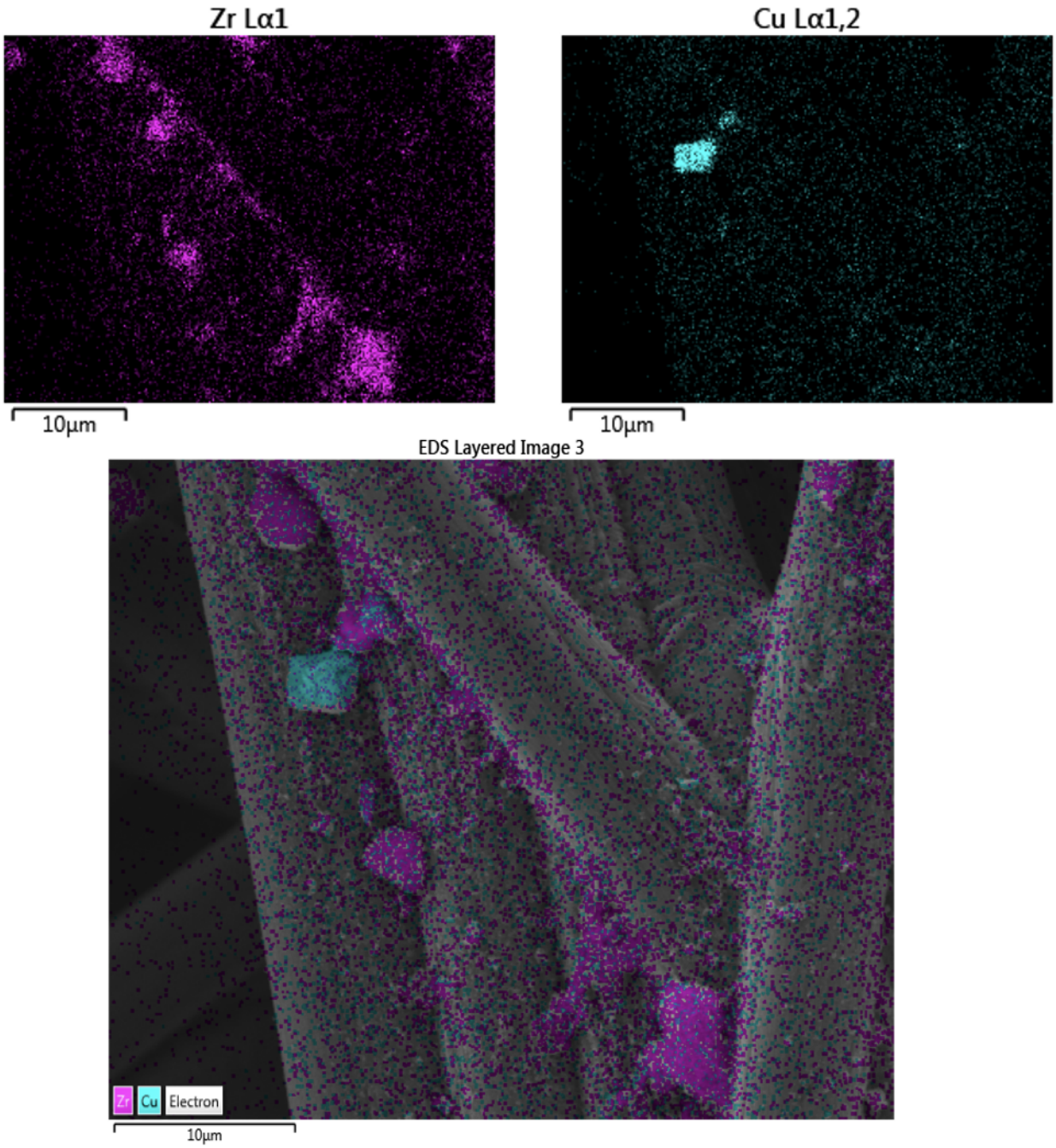

Figure S37. SEM/EDS images of UiO-66 1b (71nm), 1.5b (63nm), 2c (34nm), & HKUST-1 particles suspended in methanol then aerosolized onto carbon paper. Top left, elemental map of zirconium from UiO-66, top right elemental map of copper from HKUST-1, & bottom, SEM image overlayed with both zirconium and copper elemental maps.

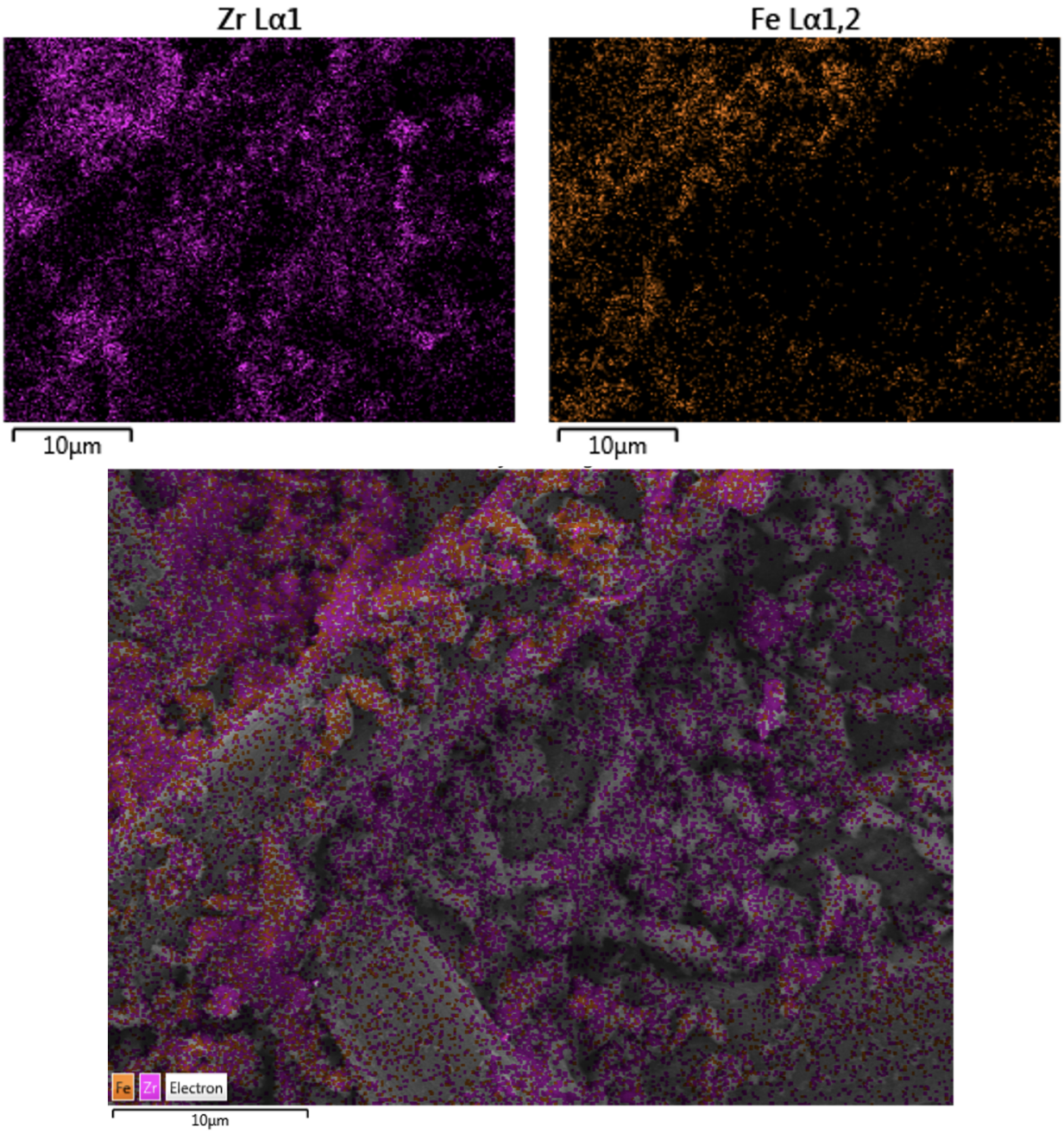

Figure S38. SEM/EDS images of UiO-66 1.5b (63nm) & Fe MIL-101 particles suspended in methanol then aerosolized onto carbon paper. Top left, elemental map of zirconium from UiO-66, top right elemental map of iron from Fe MIL-101, & bottom SEM image overlayed with both zirconium and iron elemental maps.

References

1. Shunfu du, Xuying Yu, Guoliang Liu, Mi Zhou, EI-Sayed M. El-Sayed, Zhangfeng Ju, Kongzhao Su, & Daqiang Yuan "A Straightforward Strategy for Constructing Zirconium Metallocavitands" *Cryst. Growth Des.* **2021**, 21, 692-697
2. Alexandra Antonio, Kyle Korman, Glenn Yap, & Eric Bloch "Porous metal-organic alloys based on soluble coordination cages" *Chem. Sci.* **2020**, 11, 12540
3. Gerald Decker, Zachary Stillman, Lucas Attia, Catherine Fromen, & Eric Bloch "Controlling Size, Defectiveness, and Fluorescence in Nanoparticle UiO-66 through Water and Ligand Modulation" *Chem. Mater.* **2019**, 31, 4831-4839
4. Kyle Korman, Gerald Decker, Michael Dworzak, Meaghan Deegan, Alexandra Antonio, Garrett Taggart, & Eric Bloch "Using Low-Pressure Methane Adsorption Isotherms for Higher-Throughput Screening of Methane Storage Materials" *ACS Appl. Mater. Interfaces* **2020**, 12, 40318-40327
5. Nataliya V. Maksimchuk, Konstantin A. Kovalenko, Vladimir P. Fedin, Oxana A. Kholdeeva. "Cyclohexane selective oxidation over metal-organic frameworks of MIL-101 family: superior catalytic activity and selectivity" *Chem. Commun.* **2012**, 48, 6812-14